mg, 0.242 mmol). The solution was stirred for 12 h at ambient temperature. The solvent was removed in vacuo, and ferrocene and the small excess of substrate were removed by washing the residue with ether on a medium-porosity-frit filter until the filtrate appeared colorless. The orange solid material was dissolved in dichloromethane (10 mL), and the solution was extracted with water (2 × 6 mL), dried (MgSO$_4$), filtered, and concentrated by rotary evaporation. Recrystallization from dichloromethane/ether yielded 2 (49.3 mg, 63%), pure as judged by ^{1}H NMR and IR spectroscopy.

Oxidation of 1 with 3 in NMR Tubes. In all these experiments, 1 (4.0 mg, 0.0088 mmol), 3 (ca. 2.7 mg, 0.0083 mmol), and additional reagents (2,6-lutidine, HBF$_4$·Et$_2$O, aqueous HBF$_4$ or HPF$_6$, when applicable) were loaded into an NMR tube equipped with a ground-glass joint, and the tube was attached to the vacuum line. The solvent of choice (ca. 0.4 mL) was added by vacuum transfer, and the tube was sealed under vacuum and kept at liquid-nitrogen temperature until it was inserted in the NMR probe at the preselected temperature.

For determination of absolute yields and conversions of substrate with hexamethylbenzene (HMB) as an internal standard, the following procedure was employed. A mixture of 1 (8.0 mg, 0.0175 mmol) and HMB (ca. 0.9 mg, 0.0055 mmol) was dissolved in ether (1.0 mL). The solution was distributed equally into two separate NMR tubes, and the ether was carefully removed by vacuum transfer. The oxidizing agent (and, if applicable, other reagents) were added to one tube, which was sealed under vacuum after addition of the solvent. The other tube was sealed after the addition of solvent. The relative intensities of the substrate

η^5-C$_5$H$_5$ signal and the HMB singlet provided a reference for the calculation of substrate conversion and product yields.

Constant-Current Coulometry and Preparative Electrolysis Experiments. Constant-current electrolyses with DCV monitoring of the disappearance of substrate were carried out in a H-shaped cell, the compartments of which were separated by a fritted-glass junction. A Pt-gauze working electrode was used. Solutions that contained 2.0–2.5 mM hydride 1 in 20 mL of acetonitrile/0.1 M Bu$_4$N$^+$PF$_6$$^-$ were electrolyzed with a constant current of 10 mA. The preparative electrolysis was carried out in acetonitrile/0.05 M Me$_4$N$^+$PF$_6$$^-$. A solution of 1 (41.3 mg, 0.090 mmol) in the electrolyte solution (20 mL) was electrolyzed for the time that was required for the passage of 2.0 faraday/mol of charge. The solution was concentrated by rotary evaporation, and the residue was extracted with dichloromethane (5 mL). The filtered extract was concentrated, and 2 (53.7 mg, 92.6%) was isolated as the only product after recrystallization from dichloromethane/ether. The product appeared pure by IR and ^{1}H NMR spectroscopy, and the spectra were identical with those of an authentic sample.[6a]

Low-Valent, Heterobinuclear Complexes of Rhodium and Osmium. Influence of the Coordinatively Unsaturated Rhodium Center on the Reactivity

Robert W. Hilts, Roberta A. Franchuk, and Martin Cowie*

Department of Chemistry, The University of Alberta, Edmonton, Alberta, Canada T6G 2G2

The coordinatively unsaturated complex [RhOsH(CO)$_3$(dppm)$_2$] (1) is converted smoothly to the chloro analogue [RhOsCl(CO)$_3$(dppm)$_2$] (2) in carbon tetrachloride. Compound 1 also reacts with the electrophiles HBF$_4$·Et$_2$O and [AuPPh$_3$][BF$_4$], yielding [RhOs(CO)$_3$(μ-H)(μ-X)(dppm)$_2$][BF$_4$] (X = H (3), AuPPh$_3$ (4)). The bridging AuPPh$_3$ group is readily replaced by an iodo group in the reaction of 4 with I$_2$, yielding [RhOs(CO)$_3$(μ-H)(μ-I)(dppm)$_2$][BF$_4$] (5). Reductive elimination of H$_2$ from 3, in the presence of carbon monoxide, is reversible and yields [RhOs(CO)$_4$(dppm)$_2$][BF$_4$] (6), which also reacts with the above electrophiles, yielding [RhOs(CO)$_4$(μ-X)(dppm)$_2$][BF$_4$]$_2$ (X = H (7), AuPPh$_3$ (8)). Reaction of 6 with ^{t}BuNC leads to substitution of the carbonyl on Os that is trans to the Rh–Os bond to give [RhOs(CO)$_3$-(^{t}BuNC)(dppm)$_2$][BF$_4$] (9). Compound 6 also reacts with the alkynes dimethyl acetylenedicarboxylate (DMAD) and hexafluoro-2-butyne (HFB) to give the alkyne-bridged products [RhOs(CO)$_3$(μ-CO)(μ-DMAD)(dppm)$_2$][BF$_4$] (11) and [RhOs(CO)$_3$(μ-HFB)(dppm)$_2$][BF$_4$] (13), respectively. Carbonyl loss from 11 occurs under mild conditions to yield [RhOs(CO)$_3$(μ-DMAD)(dppm)$_2$][BF$_4$] (12), analogous to compound 13. This carbonyl loss is facilitated by donation of a pair of electrons from Rh to Os with formation of a Rh→Os dative bond. Addition of anionic or neutral ligands (L) to compound 12 yields the species [RhOs(CO)$_2$L(μ-CO)(μ-DMAD)(dppm)$_2$]$^{n+}$ (n = 0, 1, respectively), in which L is coordinated on Rh and the original Rh-bound carbonyl has moved to the bridging site. Neutral ligands such as isocyanides react with 13 to yield products analogous to those obtained with 12; however, the I$^-$ and S$_2$PMe$_2$$^-$ anions (X$^-$) react with 12 with accompanying CO loss to yield [RhOsX(CO)$_2$(μ-HFB)(dppm)$_2$], in which X is bound to Rh with both carbonyls on Os. The other alkyne-bridged dicarbonyls [RhOs(CO)$_2$L(μ-RC≡CR)(dppm)$_2$]$^{n+}$ can also be obtained by heating the tricarbonyl precursors. The structure of compound 12 has been determined by X-ray techniques. This compound crystallizes with two CH$_2$Cl$_2$ molecules in the triclinic space group P$\bar{1}$ with a = 14.811 (2) Å, b = 19.250 (3) Å, c = 11.611 (1) Å, α = 103.27 (1)°, β = 94.26 (1)°, γ = 87.74 (1)°, V = 3212 (2) Å^3, and Z = 2. Refinement has converged at R = 0.041 and R_w = 0.060 on the basis of 9594 unique observations and 512 parameters varied. The geometry about Rh is essentially square planar, ignoring the Rh–Os interaction, whereas that about Os is a distorted octahedron when the dative Rh→Os interaction is taken into account. The Rh–Os separation of 2.8744 (3) Å is consistent with a single bond.

Introduction

Interest in the organometallic chemistry of heterobinuclear complexes has arisen because of the possibility of

unique chemistry resulting as a consequence of having two metals of different chemical properties in close mutual proximity[1] and also because of the related catalytic im-

plications. As part of an ongoing investigation into the chemistry of diphosphine-bridged heterobinuclear complexes,[2-7] a study into the chemistry of complexes containing one of the Fe-triad metals together with either Rh or Ir has been initiated. Metals from both triads have a well-established background of catalytic applications,[8-12] and combinations of the two have recently been successfully utilized, as for example in the use of mixed Rh–Ru complexes for ethylene glycol production[13a] and olefin hydrogenation.[13b]

Rhodium or iridium was chosen as one of the metals in these heteronuclear complexes owing to their well-established tendency to have stable, coordinatively unsaturated 16e configurations.[14a] It was thought that the presence of a coordinatively unsaturated metal adjacent to one from the Fe triad, having a tendency to remain saturated,[14b,c,d] could serve to facilitate chemistry at the latter. It was also of interest to establish what other, possibly more subtle, influences the metals might have on each other and to gain information about the nature of the metal–metal bonding involved. In complexes in which two different metals are involved, the metal–metal bonds are not purely covalent but can have significant donor–acceptor character,[1,15,16] and it was of interest to determine what effects such interactions could have on the chemistry.

In this paper we report chemistry involving the heterobinuclear complex [RhOsH(CO)$_3$(dppm)$_2$] (1), for which a donor–acceptor Os→Rh bond has previously been proposed.[4] This complex has a coordinatively unsaturated

1
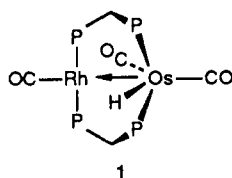
Rh center and both metals in low oxidation states; thus, it should be prone to oxidative-addition reactions. In addition, as a hydrido carbonyl complex, this and related species should prove to be valuable model systems for carbon monoxide hydrogenation in the presence of different metals.

Experimental Section

General Considerations. All solvents were dried and deoxygenated immediately before use. Sodium benzophenone was used as the drying agent for all of the solvents, except dichloromethane, which was distilled over P$_2$O$_5$. The distillations were performed under an atmosphere of prepurified argon. Rhodium(III) chloride trihydrate was purchased from Johnson Matthey Ltd., and Os$_3$(CO)$_{12}$, Ph$_2$PCH$_2$PPh$_2$ (dppm), HBF$_4$·Et$_2$O, AgBF$_4$, Au-(PPh$_3$)Cl, MeO$_2$CC≡CCO$_2$Me (DMAD), NaH, I$_2$, NaI, and [(Ph$_3$P)$_2$N]Cl were obtained from Aldrich, while Strem Chemicals was the supplier of ^{t}BuNC and ^{i}PrNC. Hexafluoro-2-butyne (HFB) was obtained from SCM Specialty Chemicals, and the 99% carbon-13-enriched carbon monoxide was purchased from Isotec Inc. The compound [RhOsH(CO)$_3$(dppm)$_2$] (1) was prepared by the published procedure.[4]

The ^{1}H, ^{1}H{^{31}P}, and ^{31}P{^{1}H} NMR spectra were recorded on a Bruker AM-400 spectrometer operating at 400.1 and 162.0 MHz for the respective nuclei. Proton-decoupled carbon-13 NMR spectra were recorded on either a Bruker AM-300 (75.5 MHz) spectrometer or the Bruker AM-400 instrument (100.6 MHz). The internal deuterated solvent served as the lock for the spectrometers. All infrared spectra were run on a Nicolet 7199 Fourier transform interferometer as solids in Nujol or dichloromethane casts on KBr. The elemental analyses were performed by the microanalytical service within the department.

Preparation of Compounds. (a) [RhOsCl(CO)$_3$(dppm)$_2$] (2). The compound [RhOsH(CO)$_3$(dppm)$_2$] (1; 0.100 g, 0.0875 mmol) was suspended in 10 mL of CCl$_4$ and stirred under argon in a sealed flask. Within 2 h all of the starting material had dissolved and a yellow-brown precipitate had formed. After 14 h of additional stirring, the solvent was removed in vacuo, leaving a yellow-brown residue, which was dissolved in 1 mL of THF. The addition of 40 mL of hexane to the resulting brown solution caused the immediate precipitation of a yellow-brown solid. The solid was washed with 2 × 20 mL of hexane and then dried under vacuum for 2 h, yielding [RhOsCl(CO)$_3$(dppm)$_2$] (2; 0.091 g, 0.077 mmol) as a brown-yellow powder, yield 88%. Anal. Calcd for C$_{53}$H$_{44}$ClO$_3$OsP$_4$Rh: C, 53.88; H, 3.75; Cl, 3.00. Found: C, 53.61; H, 4.04; Cl, 3.47.

(b) [RhOs(CO)$_3$(μ-H)$_2$(dppm)$_2$][BF$_4$] (3). The compound [RhOsH(CO)$_3$(dppm)$_2$] (1; 0.120 g, 0.105 mmol) was dissolved in 1 mL of THF, and 20 mL of Et$_2$O was added, producing a cloudy yellow solution. To this was added a colorless solution of HBF$_4$·Et$_2$O (15 μL, 0.017 g, 0.105 mmol) in 20 mL of Et$_2$O, causing the immediate precipitation of a bright yellow solid. The mixture was stirred for 30 min, the colorless supernatant discarded, and the remaining bright yellow solid washed with 3 × 20 mL of hexane. Bright yellow crystals of [RhOs(CO)$_3$(μ-H)$_2$(dppm)$_2$][BF$_4$] (3; 0.103 g, 0.083 mmol) were obtained by diffusion of Et$_2$O into a concentrated CH$_2$Cl$_2$ solution of the complex at 23 °C; yield 79%. Anal. Calcd for C$_{53}$H$_{46}$BF$_4$O$_3$OsP$_4$Rh: C, 51.56; H, 3.76. Found: C, 51.63; H, 3.90.

(c) [RhOs(CO)$_3$(μ-H)(μ-AuPPh$_3$)(dppm)$_2$][BF$_4$] (4). A solution of [Au(PPh$_3$)Cl] (0.054 g, 0.109 mmol) in 15 mL of deoxygenated acetone was added via cannula to a flask containing crystalline AgBF$_4$ (0.025 g, 0.128 mmol), causing the immediate precipitation of a colorless solid. During the next 15 min of stirring, the precipitate gradually changed from colorless through pale purple to black. The mixture was filtered, and the solvent was removed in vacuo. The colorless residue was dissolved in 15 mL of THF, and the resulting solution was added via cannula to a stirred solution of [RhOsH(CO)$_3$(dppm)$_2$] (1; 0.125 g, 0.109 mmol) in 15 mL of THF. Almost instantly the color changed from yellow to dark orange-brown and a dark brown solid precipitated. The mixture was stirred at room temperature for 30 min, after which the solvent was removed in vacuo. The brown-orange residue was redissolved in 10 mL of CH$_2$Cl$_2$, the solution was filtered, and the solvent was again removed in vacuo. Recrystallization of the resulting orange residue from CH$_2$Cl$_2$/Et$_2$O at room temperature afforded [RhOs(CO)$_3$(μ-H)(μ-AuPPh$_3$)-(dppm)$_2$][BF$_4$] (4; 0.122 g, 0.072 mmol) as orange-red crystals, yield 66%. Anal. Calcd for C$_{71}$H$_{60}$AuBF$_4$O$_3$OsP$_5$Rh: C, 50.37; H, 3.57. Found: C, 49.76; H, 3.53.

(d) [RhOs(CO)$_3$(μ-H)(μ-I)(dppm)$_2$][BF$_4$] (5). A solution of I$_2$ (0.060 g, 0.236 mmol) in 15 mL of CH$_2$Cl$_2$ was added via cannula to a stirred solution of [RhOs(CO)$_3$(μ-H)(μ-AuPPh$_3$)(dppm)$_2$][BF$_4$] (4; 0.400 g, 0.236 mmol) in 20 mL of CH$_2$Cl$_2$, causing an immediate color change from orange-red to brown. After $^1/_2$ h of stirring, the solution was filtered and the solvent was removed in vacuo,

(1) Roberts, D. A.; Geoffroy, G. L. In *Comprehensive Organometallic Chemistry*; Wilkinson, G., Stone, F. G. A., Abel, E. W., Eds.; Pergamon: Oxford U.K., 1982; Chapter 40.
(2) Vaartstra, B. A.; Cowie, M. *Organometallics* **1989**, *8*, 2388.
(3) Vaartstra, B. A.; Cowie, M. *Inorg. Chem.* **1989**, *28*, 3138.
(4) Antonelli, D. M.; Cowie, M. *Organometallics* **1990**, *9*, 1818.
(5) Antonelli, D. M.; Cowie, M. *Inorg. Chem.* **1990**, *29*, 3339.
(6) Antonelli, D. M.; Cowie, M. *Inorg. Chem.* **1990**, *29*, 4039.
(7) McDonald, R.; Cowie, M. *Inorg. Chem.* **1990**, *29*, 1564.
(8) Pruett, R. L. *Adv. Organomet. Chem.* **1979**, *17*, 1.
(9) Forster, D. *Adv. Organomet. Chem.* **1979**, *17*, 255.
(10) James, B. R. *Adv. Organomet. Chem.* **1979**, *17*, 319.
(11) Rofer-DePoorter, C. K. *Chem. Rev.* **1981**, *81*, 447.
(12) Dombek, B. D. *Adv. Catal.* **1983**, *32*, 325.
(13) (a) Dombek, B. D. *Organometallics* **1985**, *4*, 1707 and references therein. (b) Garcia, M. P.; Lopez, A. M.; Esteruelas, M. A.; Lahoz, F. J.; Oro, L. A. *J. Chem. Soc., Chem. Commun.* **1988**, 793.
(14) (a) Hughes, R. P. In *Comprehensive Organometallic Chemistry*; Wilkinson, G., Stone, F. G. A., Abel, E., Eds.; Pergamon: Oxford, 1982; Chapter 35. (b) Shriver, D. F.; Whitmire, K. H. *Ibid.*, Chapter 31. (c) Bruce, M. I. *Ibid.*, Chapter 32. (d) Adams, R. D.; Selegue, J. P. *Ibid.*, Chapter 33.
(15) Vahrenkamp, H, *Angew. Chem., Int. Ed. Engl.* **1978**, *17*, 379.
(16) Barr, R. D.; Marder, T. B.; Orpen, A. G.; Williams, I. D. *J. Chem. Soc., Chem. Commun.* **1984**, 112.

leaving a dull brown solid. The brown residue was washed with Et_2O (2 × 20 mL) and recrystallized from CH_2Cl_2/Et_2O/hexane to yield $[RhOs(CO)_3(\mu-H)(\mu-I)(dppm)_2][BF_4]\cdot^1/_2CH_2Cl_2$ (5; 0.245 g, 0.175 mmol) as brown crystals, yield 74%. The compound $[Au(PPh_3)I]$ was detected in the orange solution above the crystals of **5** by $^{31}P\{^1H\}$ NMR spectroscopy (δ 39.06 in CD_2Cl_2). Anal. Calcd for $C_{53.5}H_{46}BClF_4IO_3OsP_4Rh$: C, 45.80; H, 3.30; I, 9.05. Found: C, 45.84; H, 3.26; I, 10.31. The presence of 0.5 molar equiv of CH_2Cl_2 in the crystals was confirmed by ^1H NMR spectroscopy.

(e) $[RhOs(CO)_4(dppm)_2][BF_4]$ (6). A solution of $[RhOs(CO)_3(\mu-H)_2(dppm)_2][BF_4]$ (3; 0.100 g, 0.081 mmol) in 80 mL of CH_2Cl_2 was vigorously stirred under a slow stream of CO gas for 48 h. At the end of this time, the solvent was removed in vacuo and the resulting dark yellow residue was recrystallized from CH_2Cl_2/Et_2O to give $[RhOs(CO)_4(dppm)_2][BF_4]$ (6; 0.095 g, 0.075 mmol) as a yellow crystalline solid, yield 93%. Anal. Calcd for $C_{54}H_{44}BF_4O_4OsP_4Rh$: C, 51.44; H, 3.52. Found: C, 51.05; H, 3.45. Compound **3** can be regenerated quantitatively by passing H_2 over a CH_2Cl_2 solution of **6** for 48 h.

(f) $[RhOs(CO)_4(\mu-H)(dppm)_2][BF_4]_2$ (7). A stirred solution of $[RhOs(CO)_4(dppm)_2][BF_4]$ (6; 0.100 g, 0.079 mmol) in 10 mL of CH_2Cl_2 was charged with 15 μL of $HBF_4\cdot Et_2O$ (0.017 g, 0.105 mmol), causing an immediate color change from orange to yellow. The addition of 35 mL of Et_2O to this solution resulted in the formation of small yellow crystals of $[RhOs(CO)_4(\mu-H)(dppm)_2][BF_4]_2\cdot CH_2Cl_2$ (7; 0.103 g, 0.072 mmol), yield 91%. Anal. Calcd for $C_{55}H_{47}B_2Cl_2F_8O_4OsP_4Rh$: C, 46.08; H, 3.30; Cl, 4.95. Found: C, 46.33; H, 3.68; Cl, 5.51.

(g) $[RhOs(CO)_4(\mu-AuPPh_3)(dppm)_2][BF_4]_2$ (8). The compound $[Au(PPh_3)][BF_4]$ (0.043 g, 0.079 mmol; derived from 0.039 g of $[Au(PPh_3)Cl]$ and 0.015 g of $AgBF_4$, by the procedure outlined in part c) was dissolved in 10 mL of THF and transferred via cannula to a stirred solution of $[RhOs(CO)_4(dppm)_2][BF_4]$ (6; 0.100 g, 0.079 mmol) in 10 mL of CH_2Cl_2. Immediately the color changed from yellow to orange and a dark brown precipitate formed. After 1 h of stirring the solution was filtered to remove the gray precipitate and the solvent was removed in vacuo. Recrystallization of the dark orange residue from CH_2Cl_2/Et_2O at room temperature afforded $[RhOs(CO)_4(\mu-AuPPh_3)(dppm)_2][BF_4]_2$ (8; 0.072 g, 0.039 mmol) as orange-yellow crystals, yield 50%. Anal. Calcd for $C_{72}H_{59}AuB_2F_8O_4OsP_5Rh$: C, 47.86; H, 3.29. Found: C, 47.73; H, 3.52.

(h) $[RhOs(CO)_3(^tBuNC)(dppm)_2][BF_4]$ (9). The compound $[RhOs(CO)_4(dppm)_2][BF_4]$ (6; 0.108 g, 0.085 mmol) was dissolved in 20 mL of CH_2Cl_2 and treated with neat ^tBuNC (10 μL, 0.086 mmol). The solution was stirred for 27 h and purged with Ar for 5 min every 9 h. Following this, the solvent was removed in vacuo and the yellow residue was washed with 3 × 20 mL of Et_2O. Recrystallization from CH_2Cl_2/Et_2O at room temperature afforded $[RhOs(CO)_3(^tBuNC)(dppm)_2][BF_4]\cdot CH_2Cl_2$ (9; 0.091 g, 0.065 mmol) as bright yellow crystals, yield 76%. Anal. Calcd for $C_{59}H_{55}BCl_2F_4NO_3OsP_4Rh$: C, 50.59; H, 3.96; N, 1.00. Found: C, 50.88; H, 4.05; N, 1.17. The presence of 1 molar equiv of co-crystallized CH_2Cl_2 was confirmed by ^1H NMR spectroscopy.

(i) $[RhOs(CO)_3(\mu-CO)(\mu-DMAD)(dppm)_2][BF_4]$ (11). A solution of 10 μL of DMAD (0.012 g, 0.081 mmol) in 20 mL of THF was added via syringe to a slurry of $[RhOs(CO)_4(dppm)_2][BF_4]$ (6; 0.100 g, 0.079 mmol) in 10 mL of THF. The yellow, slightly cloudy solution gradually turned a paler shade of yellow, and a precipitate was formed during the first 1 h of stirring. After 3 h of additional stirring, the pale yellow supernatant was discarded and the yellow precipitate was washed with 20 mL of Et_2O. Recrystallization of the yellow solid from CH_2Cl_2/Et_2O at –18 °C gave yellow crystals of $[RhOs(CO)_3(\mu-CO)(\mu-DMAD)(dppm)_2][BF_4]\cdot^1/_2CH_2Cl_2$ (11; 0.084 g, 0.058 mmol), yield 73%. Anal. Calcd for $C_{60.5}H_{51}BClF_4O_8OsP_4Rh$: C, 50.28; H, 3.56. Found: C, 50.38; H, 3.58. The presence of 0.5 molar equiv of cocrystallized CH_2Cl_2 was confirmed by ^1H NMR spectroscopy. Alternatively, **11** could be prepared by bubbling CO through a solution of complex **12** in CH_2Cl_2 for 24 h. The yield of **11** from **12** after 24 h was essentially quantitative, as shown by $^{31}P\{^1H\}$ NMR spectroscopy.

(j) $[RhOs(CO)_3(\mu-DMAD)(dppm)_2][BF_4]$ (12). A suspension of $[RhOs(CO)_3(\mu-CO)(\mu-DMAD)(dppm)_2][BF_4]\cdot^1/_2CH_2Cl_2$ (11; 0.040 g, 0.028 mmol) in 15 mL of THF was refluxed under a slow stream of argon with vigorous stirring for 1 h. During this time

an orange-red product gradually precipitated from the solution. The mixture was cooled to room temperature, the pale yellow supernatant discarded, and the remaining red-orange solid dried under vacuum. Recrystallization of the residue from CH_2Cl_2/Et_2O at room temperature afforded $[RhOs(CO)_3(\mu-DMAD)-(dppm)_2][BF_4]\cdot 2CH_2Cl_2$ (12; 0.031 g, 0.020 mmol) as orange-red crystals, yield 71%. Anal. Calcd for $C_{61}H_{54}BCl_4F_4O_7OsP_4Rh$: C, 47.43; H, 3.52; Cl, 9.18. Found: C, 46.60; H, 3.50; Cl, 9.20.

(k) $[RhOs(CO)_3(\mu-HFB)(dppm)_2][BF_4]$ (13). A solution of $[RhOs(CO)_4(dppm)_2][BF_4]$ (6; 0.200 g, 0.159 mmol) in 20 mL of CH_2Cl_2 was stirred under an atmosphere of hexafluoro-2-butyne for 24 h. During this time the solution gradually changed color from yellow to orange-red. The solvent was removed, and the orange-red residue was dissolved in 2 mL of THF. The slow addition of 20 mL of Et_2O resulted in the formation of orange crystals of $[RhOs(CO)_3(\mu-HFB)(dppm)_2][BF_4]\cdot 2CH_2Cl_2$ (13; 0.216 g, 0.138 mmol), yield 87%. Anal. Calcd for $C_{59}H_{48}BCl_4F_{10}O_3OsP_4Rh$: C, 45.29; H, 3.09; Cl, 9.06. Found: C, 45.40; H, 3.18; Cl, 7.98. Proton NMR spectroscopy verified the presence of 2 molar equiv of CH_2Cl_2 in the crystals.

Reactions of Compounds 12 and 13. (a) With Isocyanides. The addition of 1 molar equiv of the appropriate isocyanide to CH_2Cl_2 solutions of either compound **12** or **13** resulted in the instantaneous formation of $[RhOs(CO)_2(RNC)(\mu-CO)(\mu-R'C\equiv CR')(dppm)_2][BF_4]$ (R = ^tBu, ^iPr; R' = CO_2Me, CF_3). The products were crystallized from CH_2Cl_2/Et_2O at room temperature.

(i) $[RhOs(CO)_2(^tBuNC)(\mu-CO)(\mu-DMAD)(dppm)_2][BF_4]$ (14): yellow crystalline solid; yield 96%. Anal. Calcd for $C_{64}H_{59}NBF_4O_7OsP_4Rh$: C, 52.72; H, 4.08; N, 0.96. Found: C, 52.51; H, 4.09; N, 0.91.

(ii) $[RhOs(CO)_2(^iPrNC)(\mu-CO)(\mu-DMAD)(dppm)_2]-[BF_4]\cdot^1/_2CH_2Cl_2$ (15): yellow crystalline solid; yield 82%. Anal. Calcd for $C_{63.5}H_{58}NBClF_4O_7OsP_4Rh$: C, 51.31; H, 3.93; N, 0.94; Cl, 2.38. Found: C, 51.48; H, 4.03; N, 0.92; Cl, 2.49.

(iii) $[RhOs(CO)_2(^tBuNC)(\mu-CO)(\mu-HFB)(dppm)_2][BF_4]$ (18): yellow-brown crystalline solid; yield 74%. Anal. Calcd for $C_{62}H_{53}NBF_{10}O_3OsP_4Rh$: C, 50.39; H, 3.61; N, 0.95. Found: C, 50.25; H, 3.31; N, 0.87.

Compound **14** was also prepared by the addition of 1 molar equiv of ^tBuNC to a CH_2Cl_2 solution of $[RhOs(CO)_3(\mu-CO)(\mu-DMAD)(dppm)_2][BF_4]$ (11), resulting in evolution of CO gas.

(b) With Anions. Acetone solutions of **12** and **13** were charged with 1 molar equiv of either NaI or $NaS_2PMe_2\cdot 2H_2O$. In all cases a color change was noted immediately. In the reactions with NaI, solids precipitated from solution over a 1-h period. After the mixtures had been stirred for 2 h, the acetone was removed under vacuum and the residues were dissolved in 10 mL of CH_2Cl_2. The resulting cloudy solutions were filtered to remove precipitated $NaBF_4$, and the solvent was again removed under vacuum. The remaining solids were washed with 2 × 20 mL of Et_2O, followed by 2 × 20 mL of hexane, and then recrystallized from CH_2Cl_2/Et_2O at room temperature.

(i) $[RhOsI(CO)_2(\mu-CO)(\mu-DMAD)(dppm)_2]$ (16): yellow crystalline solid; yield 94%. Anal. Calcd for $C_{59}H_{50}IO_7OsP_4Rh$: C, 50.08; H, 3.56; I, 8.97. Found: C, 49.85; H, 3.92; I, 8.99.

(ii) $[RhOs(\eta^1-S_2PMe_2)(CO)_2(\mu-CO)(\mu-DMAD)(dppm)_2]$ (17): yellow crystalline solid; yield 77%. Anal. Calcd for $C_{61}H_{56}O_7OsP_5RhS_2$: C, 51.84; H, 3.99. Found: C, 52.07; H, 4.30.

(iii) $[RhOsI(CO)_2(\mu-HFB)(dppm)_2]\cdot CH_2Cl_2$ (19): red crystalline solid; yield 71%. Anal. Calcd for $C_{57}H_{46}Cl_2F_6IO_2OsP_4Rh$: C, 45.89; H, 3.11; I, 8.51. Found: C, 45.60; H, 2.90; I, 8.64. The presence of 1 equiv of cocrystallized CH_2Cl_2 was confirmed by ^1H NMR spectroscopy.

(iv) $[RhOs(\eta^1-S_2PMe_2)(CO)_2(\mu-HFB)(dppm)_2]$ (20): brick red crystalline solid; yield 83%. Anal. Calcd for $C_{58}H_{50}F_6O_2OsP_5RhS_2$: C, 49.58; H, 3.59. Found: C, 50.33; H, 4.15.

Conversion of 15–17 to Dicarbonyls. Heating THF solutions of $[RhOs(CO)_2(^iPrNC)(\mu-CO)(\mu-DMAD)(dppm)_2][BF_4]$ (15), $[RhOsI(CO)_2(\mu-CO)(\mu-DMAD)(dppm)_2]$ (16), and $[RhOs(\eta^1-S_2PMe_2)(CO)_2(\mu-CO)(\mu-DMAD)(dppm)_2]$ (17) under reflux for 1 h with a continuous argon purge resulted in the loss of 1 equiv of CO and quantitative conversion to the dicarbonyl species $[RhOs(CO)_2(^iPrNC)(\mu-DMAD)(dppm)_2][BF_4]$ (21), $[RhOsI-(CO)_2(\mu-DMAD)(dppm)_2]$ (22), and $[RhOs(\eta^1-S_2PMe_2)(CO)_2(\mu-DMAD)(dppm)_2]$ (23), respectively. The isolated yields and

microanalytical data for these compounds are given below.

[RhOs(CO)$_2$(^{i}PrNC)(μ-DMAD)(dppm)$_2$][BF$_4$] (21): orange crystalline solid, recrystallized from CH$_2$Cl$_2$/Et$_2$O at 23 °C; yield 61%. Anal. Calcd for C$_{62}$H$_{57}$NBF$_4$O$_6$OsP$_4$Rh: C, 52.59; H, 4.06; N, 0.99. Found: C, 52.31; H, 4.20; N, 0.85.

[RhOsI(CO)$_2$(μ-DMAD)(dppm)$_2$] (22): pink-red crystalline solid, recrystallized from THF/Et$_2$O at 23 °C; yield 77%. Anal. Calcd for C$_{58}$H$_{50}$IO$_6$OsP$_4$Rh: C, 49.30; H, 3.57; I, 8.98. Found: C, 48.95; H, 3.,64; I, 9.13.

[RhOs(η^1-S$_2$PMe$_2$)(CO)$_2$(μ-DMAD)(dppm)$_2$] (23): orange crystalline solid, recrystallized from THF/Et$_2$O at 23 °C; yield 79%. Anal. Calcd for C$_{60}$H$_{56}$O$_6$OsP$_5$RhS$_2$: C, 52.03; H, 4.08. Found: C, 52.54; H, 4.61.

The spectroscopic data for all of the compounds are tabulated in Table I and described in detail in the Results and Discussion.

X-ray Data Collection. Orange crystals of [RhOs(CO)$_3$(μ-DMAD)(dppm)$_2$][BF$_4$]·2CH$_2$Cl$_2$ (12) were grown by diffusion of diethyl ether into a concentrated dichloromethane solution of the complex at 23 °C. Suitable crystals were mounted and flame-sealed under argon in glass capillaries to minimize decomposition and solvent loss. Diffraction data were collected on an Enraf-Nonius CAD4 diffractometer by using graphite-monochromated Mo Kα radiation. Unit-cell parameters were obtained from a least-squares refinement of the setting angles of 25 reflections in the range of $20.0° \leq 2\theta \leq 24.0°$. A triclinic cell was established by the usual peak search and reflection indexing programs, and the lack of systematic absences established the space group as either $P1$ or $P\bar{1}$. The latter was chosen and proven to be correct by the successful refinement of the structure. A cell reduction failed to find a higher symmetry cell.[17]

The intensity data were collected with use of a $\theta/2\theta$ scan technique to a maximum of $2\theta = 50.0°$. Backgrounds were measured by extending the scan 25% on either side of the calculated range. The intensities of three standard reflections were remeasured every 60 min of X-ray exposure time to check on crystal stability over the course of the data collection. Each standard lost approximately 20% of its original intensity, so a linear decomposition correction was applied to the data. The data were corrected for Lorentz and polarization effects and for absorption with use of the method of Walker and Stuart.[18] Data were processed in the usual way by using a value of 0.04 for p to downweight intense reflections.[19] A total of 9594 reflections were considered observed and were used in subsequent calculations.

Structure Solution and Refinement. The structure was solved in the space group $P\bar{1}$ by using Patterson methods to locate the metals and subsequent least-squares and difference Fourier calculations to obtain the other atom positions.[20] All hydrogen atom positions (with the exception of those in the cocrystallized CH$_2$Cl$_2$ molecules) were obtained from difference Fourier maps but were input in their idealized positions, calculated from the geometries of the attached carbon atoms with a C–H distance of 0.95 Å being used. The hydrogen atoms were given thermal parameters 20% greater than the isotropic B values of the attached carbon atoms. The refinements were carried out by full-matrix, least-squares techniques that minimized the function $\sum w(|F_o| - |F_c|)^2$, where $w = 4F_o^2/\sigma^2(F_o^2)$. The neutral atom scattering factors[21,22] and anomalous dispersion terms[23] were taken from the usual tabulations. All non-hydrogen atoms were found, and the final model converged to $R = 0.041$ and $R_w = 0.060$ with 512 parameters varied. The two cocrystallized molecules of CH$_2$Cl$_2$
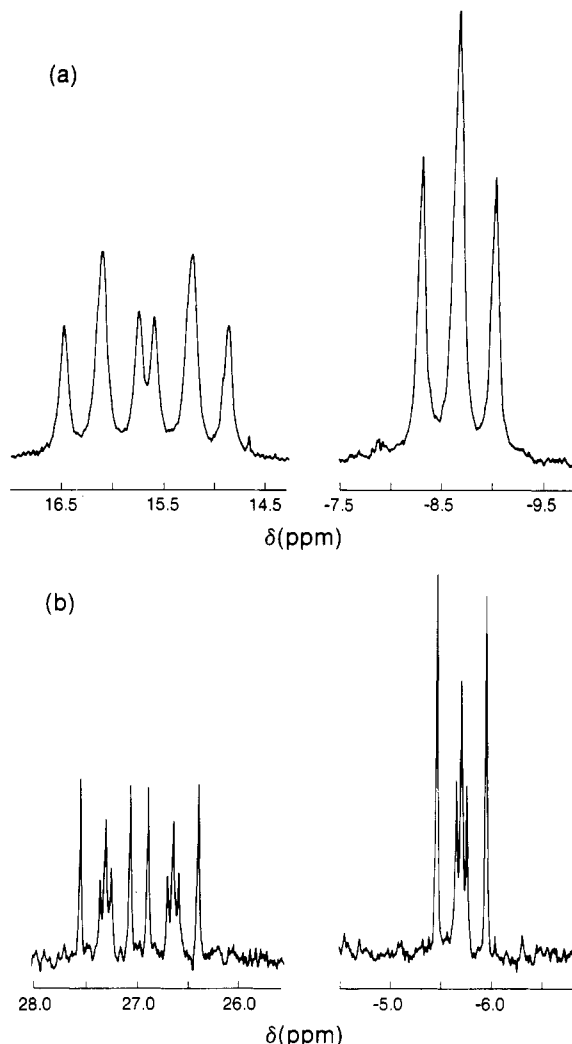
(17) The cell reduction was performed by using a modification of TRACERA II by S. L. Lawton. See: Lawton, S. L.; Jacobson, R. A. "The Reduced Cell and Its Crystallographic Applications", USAEC Ames Laboratory Report IS-1141; Iowa State University: Ames IA, April 1965.

(18) Walker, N.; Stuart, D. *Acta Crystallogr., Sect. A: Found. Crystallogr.* **1983**, *A39*, 158.

(19) Doedens, R. J.; Ibers, J. A. *Inorg. Chem.* **1967**, *6*, 204.

(20) Programs used were those of the Enraf-Nonius Structure Determination Package by B. A. Frenz, in addition to local programs by R. G. Ball.

(21) Cromer, D. J.; Waber, J. T. *International Tables for X-Ray Crystallography*; Kynoch Press: Birmingham, England, 1974; Vol. IV, Table 2.2A.

(22) Stewart, R. F.; Davidson, E. R.; Simpson, W. T. *J. Chem. Phys.* **1965**, *42*, 3175.

(23) Cromer, D. T.; Liberman, D. *J. Chem. Phys.* **1970**, *53*, 1891.

Figure 1. ^{31}P{^{1}H} NMR spectra of (a) [RhOsH(CO)$_3$(dppm)$_2$] (1) and (b) [RhOsCl(CO)$_3$(dppm)$_2$] (2), obtained at 162.0 MHz and –60 °C.

were found to have large thermal parameters, suggesting a slight disorder for these groups, and in addition, the second solvent molecule was found to be disordered about one C–Cl bond such that there were two positions for the second Cl atom, each having half-occupancy. The highest peak in the final difference Fourier map (0.94 e Å^{-3}) was located close to one of the chlorine atoms of a CH$_2$Cl$_2$ molecule. The phenyl carbons of the dppm groups, the methylene chloride carbons, and the boron atom of BF$_4^-$ were refined with isotropic thermal parameters. All other non-hydrogen atoms were refined anisotropically. A summary of the crystal data and the details of intensity measurement are provided in Table II. The positional and thermal parameters for the inner-core non-hydrogen atoms of compound 12 are collected in Table III, while selected bond lengths and angles for this structure can be found in Tables IV and V, respectively. Additional information is available as supplementary material.

Results and Discussion

In the original paper, in which we described the characterization of [RhOsH(CO)$_3$(dppm)$_2$] (1), it was noted that the bridging diphosphines may not have a trans arrangement on Os.[4] It now seems clear that this is indeed the case and that the phosphines on Os have a disposition close to that observed for the coordinatively saturated metals in [Rh$_2$(CO)$_3$(dppm)$_2$][24] and [RhIr(CO)$_3$(dppm)$_2$],[7] as diagrammed earlier for 1. In such a structure it is assumed

(24) Woodcock, C.; Eisenberg, R. *Inorg. Chem.* **1985**, *24*, 1285.

Table I. Selected Spectroscopic Data for the Compounds[a]

compd	IR, cm^{-1} [b]	$\delta(^{31}P\{^1H\})$[c]	$\delta(^{13}C\{^1H\})$[d]	$\delta(^1H)$[d]
1[e,f]	1972 (ss), 1933 (sh), 1914 (ss), 1858 (ss)	15.67 (RhP, ^1J(RhP) = 143 (Hz), −8.67 (OsP), N^h = 118 Hz	OsCO, 183.8 (t, 1 C, ^2J(PC) = 13.6 Hz, 184.9 (t, 1 C, ^2J(PC) = 13.6 Hz); RhCO, 197.6 (m, 1 C)	PCH_2P, 5.26 (bs, 2 H); OsH, −7.37 (t, 1 H, ^2J(PH) = 20 Hz)
2[e,f]	2059 (sh), 2042 (ms), 1972 (ss), 1797 (ms)	26.97 (RhP, ^1J(RhP) = 108 Hz), −5.69 (OsP), N = 79.5 Hz		PCH_2P, 5.49 (bs, 2 H)
3[e,i,j]	2035 (ss), 1974 (sb)	26.33 (RhP, ^1J(RhP) = 107 Hz), −1.36 (OsP), N = 107 Hz	OsCO, 179.84 (t, 2 C, ^2J(PC) = 8 Hz); RhCO, 186.37 (dt, 1 C, ^1J(RhC) = 76 Hz, ^2J(PC) = 17 Hz)	PCH_2P, 4.08 (m, 4 H); RhHOs, −9.95 (dtt, 2 H, ^2J(OsPH) = ^2J(RhPH) = 11.5 Hz, ^1J(RhH) = 21 Hz)
4[g,i-k]	1995 (sb), 1959 (sb), 1945 (sb)	27.79 (RhP, ^1J(RhP) = 108 Hz), −3.20 (OsP), N = 108 Hz	OsCO, 185.83 (t, 1 C, ^2J(PC) ≃ 2 Hz), 181.85 (dt, 1 C, ^2J(PC) = 10 Hz, ^3J(AuPC) = 15 Hz); RhCO, 184.12 (dt, 1 C, ^1J(RhC) = 75 Hz, ^2J(PC) = 14 Hz)	PCH_2P (AB), 4.73 (dm, 2 H), 4.39 (dm, 2 H), ^2J(HH) = 12 Hz; RhHOs, −10.16 (ddtt, 1 H, ^1J(RhH) = 21 Hz, ^2J(OsPH) = ^2J(RhPH) = 12 Hz, ^3J(AuPH) = 4 Hz)
5[g,i,j]	2050 (ms), 1973 (ss), 1956 (ss)	21.02 (RhP, ^1J(RhP) = 106 Hz), −17.36 (OsP), N = 68.5 Hz	OsCO, 172.29 (t, 1 C, ^2J(PC) = 9 Hz), 170.44 (t, 1 C, ^2J(PC) < 2 Hz); RhCO, 192.28 (dt, 1 C, ^1J(RhC) = 83 Hz, ^2J(PC) = 17 Hz)	PCH_2P (AB), 4.55 (dm, 2 H), 4.39 (dm, 2 H), ^2J(HH) = 12 Hz; RhHOs, −11.84 (dtt, 1 H, ^1J(RhH) = 23 Hz, ^2J(OsPH) = ^2J(RhPH) = 12 Hz)
6[g,i,j]	1984 (ss), 1950 (ss), 1914 (ss)	26.44 (RhP, ^1J(RhP) = 119 Hz), −7.27 (OsP), N = 110 Hz	OsCO, 179.68 (t, 1 C, ^2J(PC) = 12 Hz), 194.51 (t, 2 C, ^2J(PC) = 9 Hz); RhCO, 181.73 (dt, 1 C, ^1J(RhC) = 74 Hz, ^2J(PC) = 16 Hz)	PCH_2P, 4.31 (m, 4 H)
7[g,i,j]	2098 (ms), 2056 (ss), 1986 (mb), 1871 (mb)	27.67 (RhP, ^1J(RhP) = 104 Hz), −6.95 (OsP), N = 103 Hz		PCH_2P (AB), 4.52 (bs, 2 H), 4.25 (bs, 2 H); RhHOs, −11.00 (dtt, 1 H, J(RhH) = 22 Hz, ^2J(OsPH) = 11 Hz, ^2J(RhPH) = 8 Hz)
8[g,i,j,l]	2030 (ss), 1973 (mb), 1810 (mvb)	31.39 (RhP, ^1J(RhP) = 113 Hz), −9.15 (OsP), N = 100 Hz	OsCO, 209.00 (m, 1 C), 180.40 (m, 1 C), 173.12 (m, 1 C); RhCO, 182.62 (dm, 1 C, ^1J(RhC) = 77 Hz)	PCH_2P (AB), 5.38 (dm, 2 H), 4.28 (dm, 2 H), ^2J(HH) = 10 Hz
9[g,i,j]	1971 (bs), 1889 (mb), 2140 (ms)^m	26.08 (RhP, ^1J(RhP) = 124 Hz), −3.04 (OsP), N = 105 Hz	OsCO, 195.66 (t, 2 C, ^2J(PC) = 10 Hz); RhCO, 181.65 (dt, 1 C, ^1J(RhC) = 71 Hz, ^2J(PC) = 15 Hz)	PCH_2P, 4.32 (m, 4 H)
11[g,i,j]	2031 (ss), 1979 (sb), 1725 (sh), 1702 (mb)^n	17.76 (RhP, ^1J(RhP) = 144 Hz), −12.46 (OsP), N = 14 Hz	OsCO, 178.39 (s, 1 C), 173.94 (t, 1 C, ^2J(PC) = 16 Hz); OsCORh, 222.87 (dtt, 1 C, ^1J(RhC) = 14 Hz, ^2J(OsPC) = ^2J(RhPC) = 10 Hz); RhCO, 190.03 (dt, 1 C, ^1J(RhC) = 53 Hz, ^2J(PC) = 11 Hz)	PCH_2P (AB), 3.21 (bs, 2 H), 4.48 (bs, 2 H)
12[g,i,j]	2029 (ss), 2004 (s), 1942 (sb), 1698 (mb)^n	18.31 (RhP, ^1J(RhP) = 117 Hz), −7.50 (OsP), N = 56 Hz	OsCO, 172.02 (m, 1 C), 191.84 (s, 1 C); RhCO, 192.70 (dt, 1 C, ^1J(RhC) = 54 Hz, ^2J(PC) = 15 Hz)	PCH_2P (AB), 3.53 (dm, 2 H), 4.09 (dm, 2 H), ^2J(HH) = 9 Hz
13[e,i,j]	2037 (ss), 2021 (ss), 1963 (ss)	15.83 (RhP, ^1J(RhP) = 107 Hz), −14.01 (OsP), N = 53 Hz	OsCO, 171.08 (t, 1 C, ^2J(PC) = 4 Hz), 189.93 (s, 1 C); RhCO, 193.74 (dt, 1 C, ^1J(RhC) = 53 Hz, ^2J(PC) = 14 Hz)	PCH_2P (AB), 3.69 (dm, 2 H), 3.96 (dm, 2 H), ^2J(HH) = 10 Hz
14[e,i,j]	2041 (ss), 1978 (ss), 1711 (ms), 1691 (mb),^{n} 2147 (ms)^m	17.12 (RhP, ^1J(RhP) = 146 Hz), −11.02 (OsP), N = 16 Hz	OsCO, 175.42 (s, 1 C), 180.16 (t, 1 C, ^2J(PC) = 5 Hz); OsCORh, 232.15 (m, 1 C, ^1J(RhC) = 19 Hz, ^2J(RhPC) = 3 Hz, ^2J(OsPC) not resolved)	PCH_2P (AB), 2.71 (dm, 2 H), 4.45 (dm, 2 H), ^2J(HH) = 9 Hz
15[g,i,j]	2038 (22), 1968 (sb), 1690 (ms), 1685 (sb),^{n} 2165 (ss)^m	17.05 (RhP, ^1J(RhP) = 145 Hz), −11.16 (OsP), N = 16 Hz	OsCO, 175.39 (s, 1 C), 180.31 (t, 1 C, ^2J(PC) = 5 Hz); OsCORh, 232.02 (m, 1 C, ^1J(RhC) = 20 Hz, ^2J(RhPC) = 3 Hz, ^2J(OsPC) not resolved)	PCH_2P (AB), 2.69 (dm, 2 H), 4.45 (dm, 2 H), ^2J(HH) = 7 Hz
16[g,i]	2030 (ss), 1962 (sb), 1652 (ms), 1696 (mb)^n	10.68 (RhP, ^1J(RhP) = 149 Hz), −11.33 (OsP), N = 16 Hz	OsCO, 177.56 (s, 1 C), 182.16 (t, 1 C, ^2J(OsPC) = 7 Hz); OsCORh, 250.12 (m, 1 C, ^1J(RhC) = 22 Hz, ^2J(RhPC) = 5 Hz, ^2J(OsPC) not resolved)	PCH_2P (AB), 2.43 (dm, 2 H), 4.30 (dm, 2 H), ^2J(HH) = 8 Hz

Table I (Continued)

compd	IR, cm$^{-1\,b}$	δ(^{31}P{^{1}H})^c	δ(^{13}C{^{1}H})^d	δ(^{1}H)^d
NMR				
17^{g,i,p}	2031 (ss), 1965 (ss), 1682 (ms), 1662 (ms),^{n} 579 (ws),^{o} 601 (ms)^o	10.58 (RhP, ^1J(RhP) = 145 Hz), −12.15 (OsP), N = 16 Hz	OsCO, 177.36 (s, 1 C), 181.87 (s, 1 C), OsCORh, 245.85 (m, 1 C, ^1J(RhC) = 20 Hz, ^2J(RhPC) = 4 Hz, ^2J(OsPC) not resolved); S$_2$P(CH$_3$)$_2$, 32.66 (d, ^1J(PC) = 55 Hz)	PCH_2P (AB), 2.44 (dm, 2 H), 4.33 (dm, 2 H), ^2J(HH) = 7 Hz; S$_2$P(CH_3)$_2$, 1.29 (d, 6 H, ^2J(PH) = 13 Hz)
18^{g,i,j}	2055 (ss), 1984 (ss), 1976 (sh), 1719 (ss), 2163 (ss)^m	11.63 (RhP, ^1J(RhP) = 137 Hz), −11.50 (OsP)		PCH_2P (AB), 2.99 (dm, 2 H), 4.22 (dm, 2 H), ^2J(HH) = 8 Hz
19^{g,i}	1989 (ms), 1922 (ss)	12.50 (RhP, ^1J(RhP) = 119 Hz), −17.21 (OsP), N = 67 Hz	OsCO, 191.28 (s, 1 C), 171.41 (t, ^2J(PC) = 11 Hz)	PCH_2P (AB), 3.52 (dm, 2 H), 3.85 (dm 2 H), ^2J(HH) = 8 Hz
20^{g,i,q}	1995 (ss), 1929 (ss), 578 (ms),^{o} 599 (ms)^o	7.60 (RhP, ^1J(RhP) = 122 Hz), −16.92 (OsP), N = 32 Hz	OsCO, 171.40 (t, ^2J(PC) = 8 Hz), 189.82 (t, 1 C, ^2J(PC) < 2 Hz); S$_2$P(CH$_3$)$_2$, 32.15 (d, ^1J(PC) = 55 Hz)	PCH_2P (AB), 3.48 (dm, 2 H), 3.85 (dm, 2 H), ^2J(HH) = 8 Hz; S$_2$P(CH_3)$_2$, 1.14 (d, 6 H, ^2J(PH) = 13 Hz)
21^{g,i,j}	1930 (sb), 1875 (sb), 1694 (ss),^{n} 2164 (ss)^m	20.20 (RhP, ^1J(RhP) = 114 Hz), −9.41 (OsP), N = 64 Hz	OsCO, 192.15 (t, 1 C, ^2J(PC) = 5 Hz), 172.62 (t, 1 C, ^2J(PC) = 10 Hz)	PCH_2P (AB), 3.39 (dm, 2 H), 3.98 (dm, 2 H), ^2J(HH) = 8 Hz
22^{g,i}	1985 (ss), 1922 (ss), 1690 (ms),^{n} 1668 (ms)^n	13.48 (RhP, ^1J(RhP) = 124 Hz), −10.96 (OsP), N = 65 Hz	OsCO, 161.89 (s, 1 C), 168.31 (s, 1 C)	PCH_2P (AB), 3.42 (dm, 2 H), 4.08 (dm, 2 H), ^2J(HH) = 9 Hz
23^{g,i,r}	1930 (sb), 1874 (sb), 1687 (ss),^{n} 1667 (ss),^{n} 573 (ms),^{o} 599 (ms)^o	8.73 (RhP, ^1J(RhP) = 132 Hz), −11.84 (OsP), N = 48 Hz	OsCO, 193.70 (t, 1 C, ^2J(PC) = 5 Hz), 172.13 (t, 1 C, ^2J(PC) = 11 Hz); S$_2$P(CH$_3$)$_2$, 32.29 (d, ^1J(PC) = 47 Hz)	PCH_2P (AB), 3.83 (dm, 2 H), 4.58 (dm, 2 H), ^2J(HH) = 13 Hz; S$_2$P(CH_3)$_2$, 0.68 (d, 6 H, ^2J(PH) = 12 Hz)

^{a} Abbreviations used: for IR, (ss) strong sharp, (sb) strong broad, (ms) medium sharp, (mb) medium broad, (mvb) medium very broad, (sh) shoulder, (ws) weak sharp; for NMR, (s) singlet, (bs) broad singlet, (d) doublet, (m) multiplet, (t) triplet, (dt) doublet of triplets, (dm) doublet of multiplets, (dtt) doublet of triplets of triplets, (ddtt) doublet of doublets of triplets of triplets. ^{b} ν(CO) bands unless otherwise noted. ^{c} ^{31}P chemical shifts are quoted in parts per million relative to 85% H$_3$PO$_4$. ^{d} Carbon-13 and proton chemical shifts are quoted in parts per million relative to Si(CH$_3$)$_4$. ^{e} IR spectrum was recorded in Nujol on KBr plates. ^{f} NMR spectra were recorded in THF-d_8. ^{g} IR spectrum of CH$_2$Cl$_2$ cast. ^{h} N = |J(AB) + J(AB′)|. ^{i} NMR spectra were recorded in CD$_2$Cl$_2$. ^{j} A broad BF$_4^-$ stretch in the IR spectrum was observed at ca. 1056 cm^{-1}. ^{k} ^{31}P{^{1}H} OsAuPPh$_3$Rh: δ 56.30 (dt, ^2J(RhP) = 12 Hz, ^3J(OsPP) = 11 Hz). ^{l} ^{31}P{^{1}H} OsAuPPh$_3$Rh: δ 60.22 (1:2:2:1 multiplet). ^{m} ν(NC). ^{n} ν(CO$_2$). ^{o} ν(PS$_2$). ^{p} ^{31}P{^{1}H} η^1-S$_2$PMe$_2$: δ 53.55 (t, ^3J(RhPP) = 5 Hz). ^{q} ^{31}P{^{1}H} η^1-S$_2$PMe$_2$: δ 58.67 (s). ^{r} ^{31}P{^{1}H} η^1-S$_2$PMe$_2$: δ 69.26 (s).

Scheme I. Complexes Derived from [RhOsH(CO)$_3$(dppm)$_2$] (1)^a

[RhOsCl(CO)$_3$(dppm)$_2$] (2)

(i)

[RhOsH(CO)$_3$(dppm)$_2$] (1)

(iii)   (ii)

[RhOs(CO)$_3$(μ-H)(μ-AuPPh$_3$)(dppm)$_2$][BF$_4$] (4)   [RhOs(CO)$_3$(μ-H)$_2$(dppm)$_2$][BF$_4$] (3)

(iv)   (vi) (v)

[RhOs(CO)$_3$(μ-H)(μ-I)(dppm)$_2$][BF$_4$] (5)   [RhOs(CO)$_4$(dppm)$_2$][BF$_4$] (6)
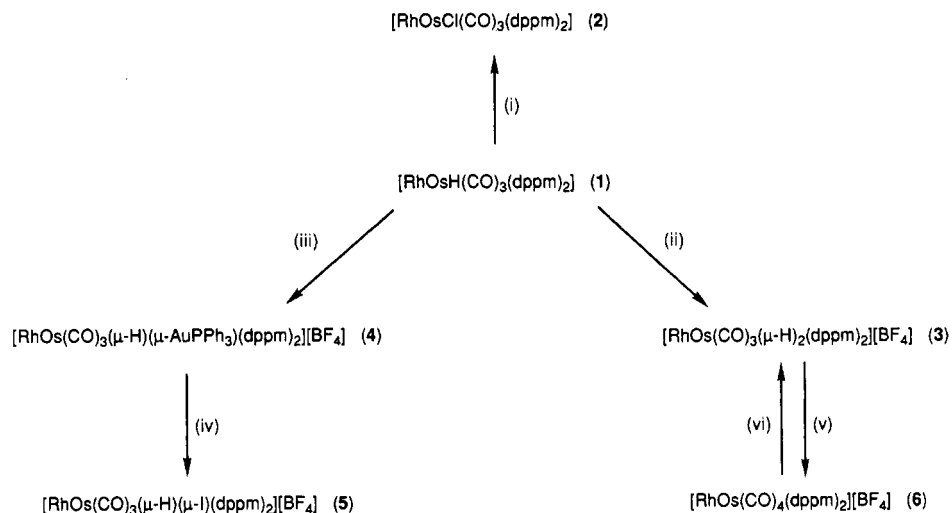
^{a} Key: (i) CCl$_4$; (ii) HBF$_4$·Et$_2$O; (iii) [AuPPh$_3$][BF$_4$]; (iv) I$_2$; (v) CO; (vi) H$_2$.

that the small hydride ligand is much less stereoactive than the large diphosphines, giving Os a pseudotetrahedral geometry if the hydride ligand and the dative Os→Rh bond are ignored. Although ignoring the dative bond appears unusual, it will be shown later that this is a reasonable approach. In fact, the geometry of the Fe center in the [FeCrH(CO)$_9$]$^-$ anion is very similar to that proposed for Os in compound 1, and it too was considered as pseudotetrahedral.[25] In support of this proposal, the ^{31}P{^{1}H}

NMR spectrum of 1, shown in Figure 1a, appears very similar to that of the isoelectronic [RhIr(CO)$_3$(dppm)$_2$][7] but quite different from those of related species in which the diphosphines have a trans arrangement at both metals (cf. Figure 1b). Although, for such a deceptively simple spectrum, simulation results are not reliable, owing to the

(25) Arndt, L. W.; Darensbourg, M. Y.; Delord, T.; Bancroft, B. T. *J. Am. Chem. Soc.* **1986**, *108*, 2617.

Table II. Crystallographic Data for
[RhOs(CO)₃(μ-DMAD)(dppm)₂][BF₄]•2CH₂Cl₂ (12)

formula	$C_{61}H_{54}BCl_4F_4O_7OsP_4Rh$
fw	1544.71
space group	$P\bar{1}$ (No. 2)
temp, °C	22
radiation (λ, Å)	graphite monochromated Mo Kα (0.710 69)
unit cell params	
a, Å	14.811 (2)
b, Å	19.250 (3)
c, Å	11.611 (1)
α, deg	103.27 (1)
β, deg	94.26 (1)
γ, deg	87.74 (1)
V, Å³	3212 (2)
Z	2
ρ(calcd), g cm⁻³	1.510
linear abs coeff (μ), cm⁻¹	24.707
range of transmissn factors	0.8713–1.1589
max 2θ, deg	50
total no. of observns (NO)	9594
no. of params varied (NV)	512
R^a	0.041
$R_w{}^b$	0.060

$^a R = \sum||F_o| - |F_c||/\sum|F_o|.$ $^b R_w = [\sum w(|F_o| - |F_c|)^2/\sum wF_o^2]^{1/2},$ where $w = 4F_o^2/\sigma^2(F_o)^2.$

Table III. Positional and Thermal Parameters for the
Inner-Core Non-Hydrogen Atoms of
[RhOs(CO)₃(μ-DMAD)(dppm)₂][BF₄]•2CH₂Cl₂ (12)^a

atom	*x*	*y*	*z*	*B*, Å²
Os	0.21885 (1)	0.30555 (1)	0.24361 (2)	2.450 (4)^{b,c}
Rh	0.22046 (3)	0.23098 (2)	−0.00097 (3)	2.466 (8)
P(1)	0.06405 (9)	0.22316 (7)	−0.0158 (1)	2.62 (3)
P(2)	0.0586 (1)	0.29224 (7)	0.2444 (1)	2.68 (3)
P(3)	0.3771 (1)	0.22417 (8)	0.0059 (1)	2.96 (3)
P(4)	0.3812 (1)	0.28953 (8)	0.2677 (1)	2.89 (3)
O(1)	0.2121 (4)	0.3172 (3)	−0.1901 (4)	6.6 (1)
O(2)	0.2143 (4)	0.4405 (2)	0.1448 (4)	5.5 (1)
O(3)	0.2292 (4)	0.3805 (3)	0.5014 (4)	6.0 (1)
O(4)	0.1889 (3)	0.0578 (2)	−0.0044 (4)	5.1 (1)
O(5)	0.3174 (3)	0.0624 (3)	0.1054 (5)	6.0 (1)
O(6)	0.1877 (4)	0.0928 (2)	0.3108 (4)	5.9 (1)
O(7)	0.2250 (3)	0.1948 (2)	0.4392 (3)	4.2 (1)
C(1)	0.2157 (4)	0.2875 (3)	−0.1168 (5)	3.6 (1)
C(2)	0.2159 (4)	0.3918 (4)	0.1852 (5)	3.6 (1)
C(3)	0.2240 (4)	0.3506 (3)	0.4037 (5)	3.6 (1)
C(4)	0.2100 (7)	−0.0162 (4)	−0.0592 (8)	6.9 (2)
C(5)	0.2489 (4)	0.0897 (3)	0.0760 (5)	3.4 (1)
C(6)	0.2263 (4)	0.1672 (3)	0.1242 (5)	2.6 (1)
C(7)	0.2204 (4)	0.1961 (3)	0.2382 (5)	2.6 (1)
C(8)	0.2101 (4)	0.1542 (3)	0.3299 (5)	3.4 (1)
C(9)	0.2159 (7)	0.1602 (4)	0.5354 (6)	6.3 (2)
C(10)	0.0165 (4)	0.2204 (3)	0.1223 (5)	2.8 (1)
C(11)	0.4282 (4)	0.2187 (3)	0.1516 (5)	3.1 (1)

^{a} The parameters for the phenyl groups, the $BF_4{}^-$ anion, and the CH_2Cl_2 solvent molecules are given in the supplementary material. ^{b} All atoms given in this table were refined anisotropically. ^{c} Anisotropically refined atoms are given in the form of the isotropic equivalent displacement parameter, defined as $^4/_3[a^2\beta(1,1) + b^2\beta(2,2) + c^2\beta(3,3) + ab(\cos\gamma)\beta(1,2) + ac(\cos\beta)\beta(1,3) + bc(\cos\alpha)\beta(2,3)].$

paucity of lines observed, we have obtained a value of $^2J_{P-Os-P} = 30$ Hz for the coupling between the two phosphorus nuclei bound to Os in compound 1.[26] This value is much lower than that expected (ca. 170 Hz)[27] for a trans

(26) In our simulations the value $^2J(POsP)$ consistently falls close to 30 Hz for those sets of coupling constants that give rms values below 0.05.

(27) (a) Jenkins, J. A. M.Sc. Thesis, Dalhousie University, 1984. (b) Hilts, R. W.; Cowie, M. Unpublished work, University of Alberta.

Table IV. Selected Bond Lengths (Å) for
[RhOs(CO)₃(μ-DMAD)(dppm)₂][BF₄]•2CH₂Cl₂ (12)^a

Os–Rh	2.8744 (3)	O(2)–C(2)	1.140 (5)
Os–P(2)	2.398 (1)	O(3)–C(3)	1.147 (5)
Os–P(4)	2.416 (1)	O(4)–C(4)	1.453 (6)
Os–C(2)	1.930 (4)	O(4)–C(5)	1.302 (5)
Os–C(3)	1.859 (5)	O(5)–C(5)	1.187 (5)
Os–C(7)	2.092 (4)	O(6)–C(8)	1.207 (5)
Rh–P(1)	2.318 (1)	O(7)–C(8)	1.337 (5)
Rh–P(3)	2.315 (1)	O(7)–O(9)	1.442 (6)
Rh–C(1)	1.910 (4)	C(5)–C(6)	1.503 (5)
Rh–C(6)	2.103 (4)	C(6)–C(7)	1.321 (5)
O(1)–C(1)	1.125 (5)	C(7)–C(8)	1.495 (5)

^{a} Parameters for the $BF_4{}^-$ anion, the CH_2Cl_2 molecules, and bonds within the dppm ligands are given in the supplementary material.

arrangement and is more consistent with the cis orientation proposed.

Compound 1 can be readily transformed into a series of related complexes as summarized in Scheme I. In carbon tetrachloride, compound 1 is transformed smoothly to the analogous chloride [RhOsCl(CO)₃(dppm)₂] (2). Consistent
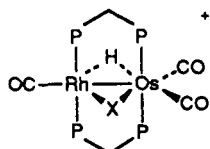

2
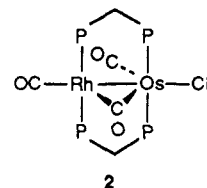
with the previous argument regarding the small size of the hydrido ligand in 1, its replacement by the larger chloride ligand apparently causes a slight structural change. Now the ^{31}P{^{1}H} NMR spectrum, shown in Figure 1b, is consistent with a trans arrangement of phosphines on both metals, and a simulation of this spectrum yields a tentative value for $^2J_{P-Os-P}$ of ca. 90 Hz. The relative positions of the two ^{31}P chemical shifts are consistent with previous observations in which phosphorus nuclei bound to third-row metals were found at higher field than those bound to metals of the second row.[2-7,28] The IR spectrum of 2 differs from that of 1 in that there is one higher (2042 cm⁻¹) and one lower (1797 cm⁻¹) frequency carbonyl stretch. In the ^{1}H NMR spectrum only one signal appears for the dppm methylene protons, suggesting a symmetric structure in which Cl is opposite the Os–Rh bond. However, the two very different carbonyl stretches noted imply two very different environments and the low stretch suggests a structure in which one of the carbonyls is bridging, or at least in a semibridging position, accepting electron density from the electron-rich Rh center. These data together suggest a fluxional process that exchanges the two carbonyls on Os. Although the low-temperature limiting spectrum was not obtained, this is not too surprising since exchange of the two carbonyl environments should occur readily by a slight wagging about the Os–Rh bond, bringing the terminal carbonyl to a bridging position and vice versa. A ^{13}C{^{1}H} NMR spectrum could not be obtained owing to the low solubility of 2.

Protonation of compound 1, with use of HBF₄·Et₂O, results in an accompanying movement of the terminal hydride on Os to the bridging position, yielding [RhOs(CO)₃(μ-H)₂(dppm)₂][BF₄] (3), in which both hydride ligands bridge the metals in equivalent chemical environments. The ^{31}P{^{1}H} NMR spectrum of 3 shows a multiplet pattern at δ −1.36 for the osmium-bound phosphorus nuclei

(28) See for example: McEwan, D. M.; Pringle, P. G.; Shaw, B. L. *J. Chem. Soc., Chem. Commun.* 1982, 859.

X = H (3), AuPPh₃ (4), I (5)

and a doublet of multiplets at δ 26.33 for those on rhodium (see Table I). This pattern is typical of an AA'BB'X spin system in which two trans dppm groups bridge rhodium and another metal[28] and is quite similar to that shown in Figure 1b for compound 2. The high-field multiplet at δ -9.95 in the ¹H NMR spectrum is integrated as two hydrogens and has been shown, by selective ³¹P decoupling experiments, to be a doublet of triplets of triplets, displaying coupling to Rh and to both chemically inequivalent sets of phosphorus nuclei, thereby unequivocally establishing that these hydrides bridge the metals. The single resonance observed for the dppm methylene protons is consistent with a structure having mirror symmetry about the RhOsP₄ plane, in which these protons exchange between axial and equatorial orientations.[29] In the ¹³C{¹H} NMR spectrum the carbonyl group on Rh appears as a doublet of triplets at δ 186.37, displaying coupling to Rh and the two adjacent phosphorus nuclei, whereas the two carbonyls on Os appear as a triplet of twice the intensity at δ 179.84, with coupling to only the adjacent phosphorus atoms. All data are consistent with the structure shown, which is analogous to that previously proposed for the isoelectronic species [RhRe(CO)₃(μ-H)₂(dppm)₂].[6]

Compound 1 also reacts with [Au(PPh₃)][BF₄] to yield the structurally analogous trinuclear cluster [RhOs-(CO)₃(μ-H)(μ-AuPPh₃)(dppm)₂][BF₄] (4). On the basis of the isolobality[30] of AuPPh₃⁺ and H⁺, the structure proposed for 4 is not unexpected, although differences in reactivity between these two electrophiles have been noted.[31,32] The ³¹P{¹H} NMR spectrum of 4 displays two dppm resonances having chemical shifts very similar to those of 3 and a AuPPh₃ resonance in the expected region. However, this spectrum is somewhat more complex than that of 3 owing to the additional PPh₃ group, which gives rise to an AA'BB'MX spin system. Surprisingly perhaps, the PPh₃ resonance displays coupling to Rh (²J_{Rh-P(Au)} = 12 Hz) and to the phosphorus nuclei on Os (³J_{P(Os)-P(Au)} = 11 Hz), suggesting that the AuPPh₃ group bridges the metals; however, this group does not display coupling to the phosphorus nuclei on Rh. These results, however, are consistent with those of Schiavo and co-workers, who have observed coupling (³J_{P(Rh)-P(Au)}) between the Au-bound phosphorus atom and those on Rh of less than 1 Hz in [Rh₂Cp₂(μ-CO)(μ-AuPPh₃)(dppm)][BF₄].[32] In the ¹H NMR spectrum of 4 the hydride resonance appears at a shift (δ -10.16) similar to that of 3, although it displays a more complex pattern owing to additional coupling to the phosphorus of the PPh₃ group. Consistent with the lower symmetry of 4, the dppm methylene protons appear as an AB quartet with additional fine structure arising from coupling to the dppm phosphorus nuclei, and three carbonyl resonances are observed in the ¹³C{¹H} NMR spectrum. The ¹³C resonance at δ 181.85 is a doublet of triplets, displaying coupling to the Os-bound and the

Au-bound phosphorus nuclei, indicating that this Os-bound carbonyl is trans to the AuPPh₃ group, the resonance at δ 185.83 is a triplet with coupling only to the Os-bound phosphorus atoms, and that at δ 184.12 is a doublet of triplets with coupling to Rh and to its attached phosphorus nuclei.

The corresponding iodo-bridged complex [RhOs(CO)₃-(μ-H)(μ-I)(dppm)₂][BF₄] (5) can be readily prepared by the reaction of 4 with I₂, yielding [Au(PPh₃)I] as the other product. Although the phosphorus chemical shifts for 5 are significantly different from those of 3 and 4, we favor an analogous structure for 5, in which the iodo and hydrido groups bridge the metals, as shown earlier. The large chemical shift differences, particularly involving the Os-bound phosphorus atoms, is possibly not surprising since the iodo ligand is electronically quite different from the H or AuPPh₃ groups, being capable of donating two additional electrons when bridging. Compound 5 is analogous to the isoelectronic compound [RhRe(CO)₃(μ-H)(μ-Cl)-(dppm)₂][6] and also to the closely related thiolato-bridged species [RhRe(CO)₃(μ-H)(μ-SEt)(dppm)₂], the latter of which has been shown by an X-ray study[5] to have a structure as proposed for 5.

Reaction of 3 with carbon monoxide results in the reductive elimination of H₂ and its replacement by an additional carbonyl group to give [RhOs(CO)₄(dppm)₂][BF₄] (6). The structure of 6 is believed to be analogous to that

6
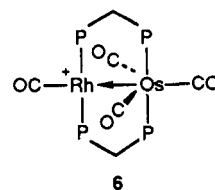
of the isoelectronic species [RhRe(CO)₄(dppm)₂], the structure of which was established crystallographically.[4] Replacement of H₂ by CO results in little change in the chemical shift for the phosphorus atoms on Rh, but the Os-bound phosphorus resonance is shifted upfield by approximately 6 ppm. The ¹³C{¹H} NMR spectrum of 6 shows two triplets in a 2:1 intensity ratio at δ 194.51 and 179.68, respectively, and a doublet of triplets at δ 181.73 (¹J_{Rh-C} = 74 Hz, 1 C). For the isoelectronic, neutral RhRe species the resonance for the Rh-bound carbonyl remains in almost the same position (δ 181.5), whereas those on Re are shifted downfield to δ 217.6 and 206.3. This large shift difference between the Os- and the Re-bound carbonyls probably results from greater π back-donation to the rhenium carbonyls, giving rise to changes in the paramagnetic screening constant for these CO's.[33,34] Such a view suggests that the Rh centers in both compounds are similar, consistent with our interpretation of these compounds as containing Rh(I)/Re(-I) and Rh(I)/Os(0) centers,[4] in which the Re(-I) center is a better electron donor to the carbonyls, and is supported by the red shift of the carbonyl stretches in the RhRe compound compared to those in 6. Compound 3 can be regenerated from 6 under a dihydrogen atmosphere, showing that the oxidative-addition and reductive-elimination cycle is reversible.

Although carbonyl exchange over the two metal centers in 6 is not observed at ambient temperature, exposure to ¹³CO results in total enrichment of all positions in less than 1 h. Presumably this occurs via a pentacarbonyl inter-

(29) See for example: Balch, A. L.; Hunt, C. T.; Lee, C.-L.; Olmstead, M. M.; Farr, J. P. *J. Am. Chem. Soc.* **1981**, *103*, 3764.
(30) Evans, D. G.; Mingos, D. M. P. *J. Organomet. Chem.* **1982**, *232*, 171.
(31) Hilts, R. W.; Cowie, M. *Inorg. Chem.* **1990**, *29*, 3349.
(32) Schiavo, S. L.; Bruno, G.; Nicolo, F.; Piraino, P.; Faraone, F. *Organometallics* **1985**, *4*, 2091 and references therein.

(33) Brown, D. A.; Chester, J. P.; Fitzpatrick, N. J.; King, I. J. *Inorg. Chem.* **1977**, *16*, 2497.
(34) Gansow, O. A.; Schexnayder, D. A.; Kimura, B. Y. *J. Am. Chem. Soc.* **1972**, *94*, 3406.

Table V. Selected Bond Angles (deg) for [RhOs(CO)₃(μ-DMAD)(dppm)₂][BF₄]•2CH₂Cl₂ (12)[a]

Bond Angles

Rh–Os–P(2)	92.04 (2)	P(1)–Rh–P(3)	173.18 (4)	Os–P(4)–C(91)	117.8 (1)
Rh–Os–P(4)	90.27 (3)	P(1)–Rh–C(1)	91.3 (1)	C(4)–O(4)–C(5)	115.6 (4)
Rh–Os–C(2)	85.9 (1)	P(1)–Rh–C(6)	88.8 (1)	C(8)–O(7)–C(9)	116.1 (4)
Rh–Os–C(3)	176.5 (1)	P(3)–Rh–C(1)	91.8 (1)	Rh–C(1)–O(1)	175.8 (4)
P(2)–Os–P(4)	163.54 (4)	P(3)–Rh–C(6)	87.9 (1)	Os–C(2)–O(2)	176.4 (4)
P(2)–Os–C(2)	98.0 (1)	C(1)–Rh–C(6)	179.0 (2)	Os–C(3)–O(3)	177.3 (4)
P(2)–Os–C(3)	90.4 (1)	Rh–P(1)–C(10)	113.8 (1)	O(4)–C(5)–O(5)	124.5 (4)
P(2)–Os–C(7)	82.3 (1)	Rh–P(1)–C(21)	108.9 (1)	O(4)–C(5)–C(6)	113.3 (4)
P(4)–Os–C(2)	98.4 (1)	Rh–P(1)–C(31)	120.8 (1)	O(5)–C(5)–C(6)	122.2 (4)
P(4)–Os–C(3)	86.7 (1)	Os–P(2)–C(10)	111.9 (1)	Rh–C(6)–C(5)	114.9 (3)
P(4)–Os–C(7)	82.9 (1)	Os–P(2)–C(41)	117.6 (1)	Rh–C(6)–C(7)	120.9 (3)
C(2)–Os–C(3)	96.1 (2)	Os–P(2)–C(41)	118.2 (3)	C(5)–C(6)–C(7)	123.7 (3)
C(2)–Os–C(7)	158.4 (2)	Os–P(2)–C(51)	115.9 (1)	Os–C(7)–C(6)	102.7 (3)
C(3)–Os–C(7)	105.5 (2)	Rh–P(3)–C(11)	112.9 (1)	Os–C(7)–C(8)	133.2 (3)
Os–Rh–P(1)	91.19 (3)	Rh–P(3)–C(61)	106.7 (1)	C(6)–C(7)–C(8)	123.9 (3)
Os–Rh–P(3)	92.71 (3)	Rh–P(3)–C(71)	121.1 (1)	O(6)–C(8)–C(7)	123.1 (4)
Os–Rh–C(1)	117.2 (1)	Os–P(4)–C(11)	113.9 (1)	O(6)–C(8)–C(7)	125.9 (4)
Os–Rh–C(6)	63.7 (1)	Os–P(4)–C(81)	114.1 (1)	O(7)–C(8)–C(7)	111.0 (4)

Torsion Angles

C(1)–Rh–Os–C(2)	−1.3 (3)	P(1)–Rh–Os–P(2)	4.50 (5)
C(6)–Rh–Os–C(7)	−2.3 (2)	P(3)–Rh–Os–P(4)	−6.22 (5)

[a] Numbers in parentheses are estimated standard deviations in the least significant digits.

**Scheme II. Complexes Derived from [RhOs(CO)₄(dppm)₂][BF₄] (6)[a]**
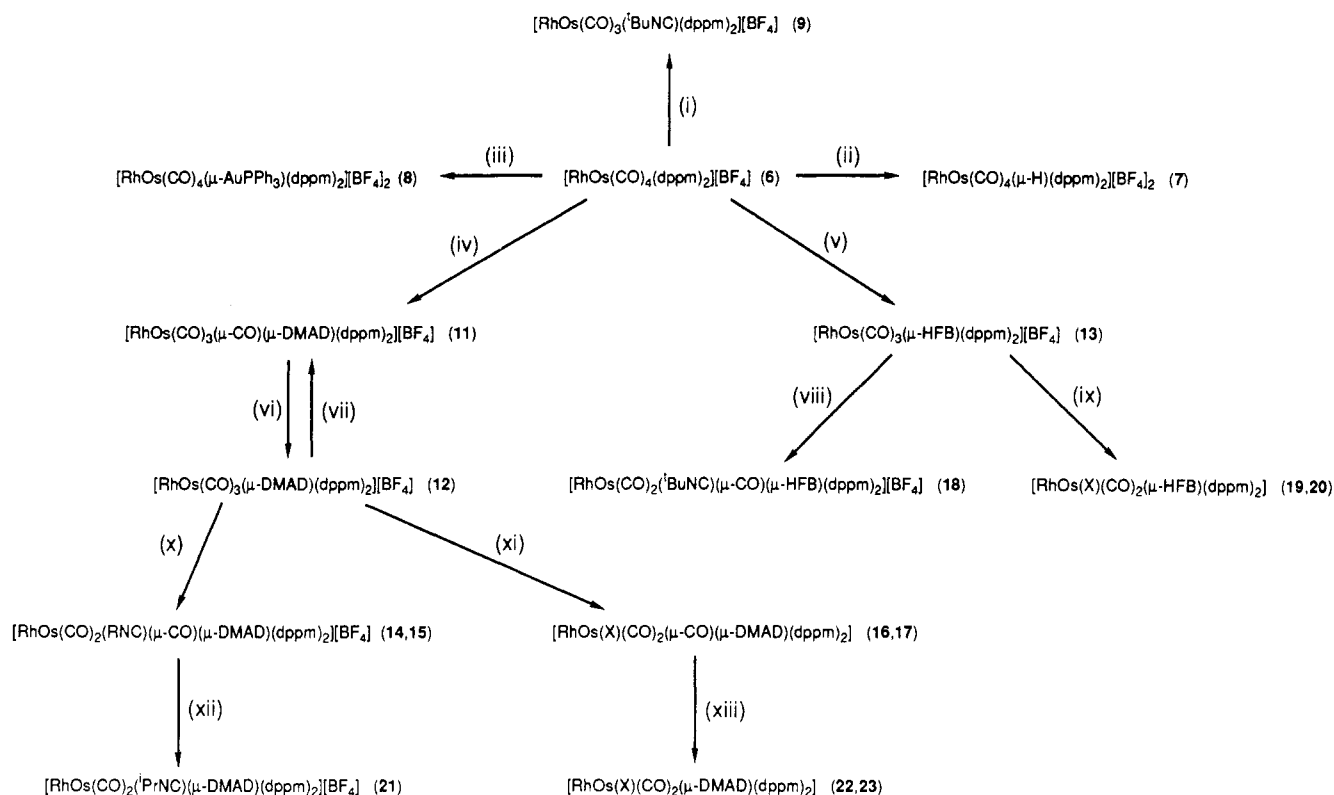
[a] Key: (i) ¹BuNC; (ii) HBF₄·Et₂O; (iii) [AuPPh₃][BF₄]; (iv) H₃CO₂CC≡CCO₂CH₃; (v) F₃CC≡CCF₃; (vi) refluxing THF; (vii) CO; (viii) ¹BuNC; (ix) NaX (X = I for 19, S₂PMe₂ for 20; (x) RNC (R = ¹Bu for 14, ¹Pr for 15); (xi) NaX (X = I for 16, S₂PMe₂ for 17; (xii) refluxing THF for R = ¹Pr; (xiii) refluxing THF (X = I for 22, S₂PMe₂ for 23).

mediate such as [RhOs(CO)₅(dppm)₂]⁺, although such a species was not observed. In the related RhRe system the labile pentacarbonyl [RhRe(CO)₅(dppm)₂] was observed and was found to undergo rapid carbonyl exchange over both metals.[6] Further support for the proposed pentacarbonyl "RhOs" intermediate comes from the analogous IrOs system, in which the species [IrOs(CO)₅(dppm)₂][BF₄] was isolated and characterized.[35]

The compounds derived from compound **6** are summarized in Scheme II. Treatment of **6** with HBF₄·Et₂O or [AuPPh₃][BF₄] yields the respective dicationic species [RhOs(CO)₄(μ-H)(dppm)₂][BF₄]₂ (**7**) or [RhOs(CO)₄(μ-AuPPh₃)(dppm)₂][BF₄]₂ (**8**). The most obvious change brought about by the addition of the electrophiles to **6** is a shift of the carbonyl stretches to higher frequency, consistent with the increased positive charge on the complexes. The ¹³C{¹H} NMR spectra of **7** and **8** each display three Os–carbonyl resonances and one for the carbonyl on Rh, and the ³¹P{¹H} NMR spectra are essentially as ex-

(35) Hilts, R. W.; Franchuk, R. A.; Cowie, M. *Organometallics*, in press.

pected and are not unlike those of **3** and **4**, respectively. The ^1H NMR spectrum of **7** shows a high-field multiplet at δ -11.00, displaying coupling to Rh and to all four phosphorus nuclei, indicating that the hydride bridges the two metals. On the basis of these data and on the structure determination of the isoelectronic species [RhRe(CO)$_4$(μ-H)(dppm)$_2$][BF$_4$],[6] the structure

X = H (**7**), AuPPh$_3$ (**8**)
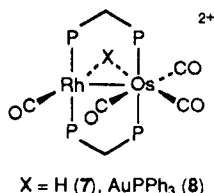
is proposed for the cations of **7** and **8**, in which the Rh center is essentially square planar and the Os is octahedral (ignoring the Rh–Os interaction).

Compound **6** also reacts with ^tBuNC, resulting in the substitution of one carbonyl group to give [RhOs(CO)$_3$-(^tBuNC)(dppm)$_2$][BF$_4$] (**9**). This product shows a stretch for the terminal isocyanide ligand at 2140 cm^{-1} in addition to two terminal carbonyl stretches (1889, 1971 cm^{-1}). The isocyanide ligand can be established as occupying the site on Os opposite the Rh–Os bond, since the $^{13}C\{^1H\}$ NMR spectrum shows one resonance for the Rh-bound carbonyl (δ 181.65), displaying the expected coupling to Rh and two phosphorus nuclei, and a resonance of twice the intensity (δ 195.66) corresponding to the two chemically equivalent carbonyls bound to Os, displaying coupling only to two phosphorus atoms. Further support for the symmetrical structure of **9** comes from the ^1H NMR spectrum, which displays only a single resonance for the methylene protons, as observed for compounds **2** and **3**. Although it is tempting to discuss this substitution in terms of a trans effect of the Rh–Os bond, since the ^tBuNC ligand apparently replaces the carbonyl originally in this site, it appears more likely that initial attack by ^tBuNC occurs at Rh to give an intermediate (**10a**), not unlike the pentacarbonyl

10a

10b   **9**
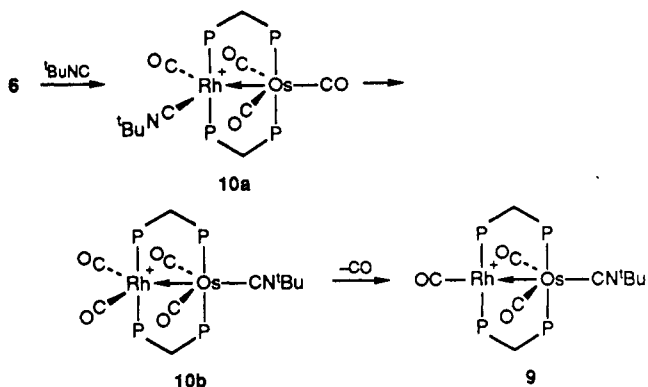
species proposed earlier. This species could be envisioned as undergoing a rapid rearrangement to a species such as **10b**, which loses CO from Rh. The second carbonyl on Rh in a species such as **10b** would be expected to be very labile, as witnessed by our failure to observe the pentacarbonyl species mentioned earlier. Complexes such as **9** and **10b**, having the ^tBuNC ligand opposite the Os$\rightarrow$Rh bond, may be favored for both steric and electronic reasons. In this position the bulky ^tBu moiety interacts only with the phenyl substituents on one end of the dppm groups, and since ^tBuNC is a better σ-donor[36] than a carbonyl, it should stabilize the proposed Os$\rightarrow$Rh dative interaction (the in-

crease in the CN stretching frequency from the value of 2125 cm^{-1} observed in free ^tBuNC is consistent with this group functioning mainly as a σ-donor). In complexes proposed to have M$\rightarrow$M' dative bonds, ligands that are stronger σ-donors have previously been observed to occupy the site on the donor metal opposite the M$\rightarrow$M' bond.[25,37,38]

Compound **6** also reacts with dimethyl acetylenedicarboxylate (DMAD) but does not initially yield the substitution product; instead, it yields the addition product [RhOs(CO)$_3$(μ-CO)(μ-DMAD)(dppm)$_2$][BF$_4$] (**11**). The $^{31}P\{^1H\}$ NMR spectrum is again consistent with an AA'BB'X spin system in which the diphosphines are mutually trans and bridge the metals, and the ^1H NMR spectrum shows two different methyl environments for the bridging DMAD ligand as well as two different resonances for the dppm methylene protons. The $^{13}C\{^1H\}$ NMR spectrum displays four carbonyl resonances. Two resonances (δ 178.39, 173.94) show coupling to only the Os-bound phosphorus nuclei and so are clearly terminally bound to Os, another (δ 190.03) shows coupling to Rh ($^1J_{Rh-C}$ = 53 Hz) and to the Rh-bound phosphorus nuclei, indicating that this group is terminally bound to Rh, and the fourth resonance (δ 222.87) displays coupling to Rh ($^1J_{Rh-C}$ = 14 Hz) and to all four phosphorus nuclei, suggesting that it bridges both metals. This suggestion is supported by the low-field shift of the ^{13}C resonance for this carbonyl, which is in a region typical of bridging carbonyls, and by the low IR stretch (ca. 1725 cm^{-1}) for this group. Two different methyl resonances (δ 50.30, 49.27) are also observed for the DMAD group in the $^{13}C\{^1H\}$ NMR spectrum. On the basis of these data and on the overwhelming tendency for alkynes to bridge the metals in related complexes,[39,40] the structure

11   **12**

R = CO$_2$Me
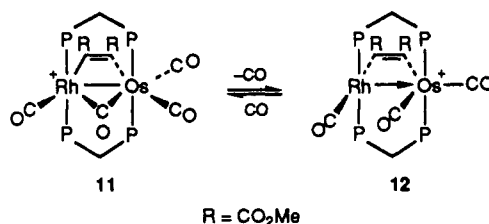
in which the alkyne bridges the two metals parallel to the Rh–Os axis, is proposed. The formulation of **11** as containing a ketonic carbonyl, with no accompanying Rh–Os bond, is consistent with the IR stretch for this group, which is partially obscured by the DMAD carbonyl stretches. Furthermore, the Rh center in such a formulation is isoelectronic with those in the related species [Rh$_2$Cl$_2$(μ-CO)(μ-DMAD)(dppm)$_2$], which was shown by an X-ray structure determination to have a ketonic carbonyl in which this carbon can be viewed as sp^2 hybridized.[41] Compound **11** would then be formulated as a Rh(III)/Os(II) species, in which the bridging alkyne and the bridging carbonyl are considered as dianionic ligands. This

(36) Treichel, P. M. *Adv. Organomet. Chem.* **1973**, *11*, 21.

(37) Breen, M. J.; Shulman, P. M.; Geoffroy, G. L.; Rheingold, A. L.; Fultz, W. C. *Organometallics* **1984**, *3*, 782.

(38) Einstein, F. W. B.; Jones, T.; Pomeroy, R. K.; Rushman, P. *J. Am. Chem. Soc.* **1984**, *106*, 2707.

(39) Hoffman, D. M.; Hoffmann, R.; Fisel, C. R. *J. Am. Chem. Soc.* **1982**, *104*, 3858 and references therein.

(40) For some leading references see: (a) McKeer, I. R.; Sherlock, S. J.; Cowie, M. *J. Organomet. Chem.* **1988**, *352*, 205. (b) Mague, J. T. *Organometallics* **1986**, *5*, 918. (c) Dickson, R. S.; Pain, G. N. *J. Chem. Soc., Chem. Commun.* **1979**, 277. (d) Berry, D. H.; Eisenberg, R. *Organometallics* **1987**, *6*, 1796. (e) Lee, C.-L.; Hunt, C. T.; Balch, A. L. *Inorg. Chem.* **1981**, *20*, 2498. (f) Muetterties, E. L.; Pretzer, W. R.; Thomas, M. G.; Beier, B. F.; Thorn, D. L.; Day, V. W.; Anderson, A. B. *J. Am. Chem. Soc.* **1978**, *100*, 2090. (g) El Amane, M.; Mathieu, R.; Poilblanc, R. *Organometallics* **1983**, *2*, 1618.

(41) Cowie, M.; Southern, T. G. *Inorg. Chem.* **1982**, *21*, 246.

compound can also be viewed as a model intermediate in the above conversion of 10a to 10b, with the added ligand and one carbonyl from Os in the process of exchanging metals.

Refluxing compound 11 in THF results in the loss of one carbonyl group from Os to yield $[RhOs(CO)_3(\mu\text{-}DMAD)(dppm)_2][BF_4]$ (12). The $^{13}C\{^1H\}$ NMR spectrum clearly establishes that carbonyl loss from Os has occurred, since only three carbonyl resonances of equal intensity are observed, with only the lowest field resonance displaying Rh coupling. Carbonyl loss and the resulting coordinative unsaturation at Os could in principle be remedied by rotation of the alkyne to an orientation perpendicular to the Rh–Os axis, as has previously been observed in related systems.[40c,42] Such a rotation transforms the two-electron-donor alkyne (viewed as a neutral group) to a four-electron donor. However, spectroscopic data in the present case suggest that alkyne rotation has not occurred, since the ^1H NMR spectrum of 12 displays two methyl resonances, which is not expected for the perpendicular binding mode, in which both methyls should be equivalent, and the $^{31}P\{^1H\}$ NMR spectrum still appears typical of an AA′BB′X spin system in which the diphosphines are mutually trans (the perpendicular alkyne binding mode would be accompanied by a change to a mutually cis phosphine alignment).[40d,43] This proposal has been confirmed by the X-ray structure determination of compound 12 (vide infra). Carbonyl loss from 11 is reversible; therefore, under a CO atmosphere compound 11 is regenerated from 12.

In the reaction of 6 with hexafluoro-2-butyne (HFB) the tetracarbonyl species analogous to 11 is not observed; instead, only the tricarbonyl $[RhOs(CO)_3(\mu\text{-}HFB)(dppm)_2][BF_4]$ (13), analogous to 12, is obtained. More facile carbonyl loss from the presumed HFB-bridged tetracarbonyl intermediate than from the DMAD analogue (11) is not surprising since the greater group electronegativity of CF_3 compared to CO_2Me[44] makes HFB a better π-acceptor, which then competes more effectively for π-electron density, resulting in greater labilization of a carbonyl group.

It appears that for these alkyne-bridged heterobinuclear complexes the coordinatively unsaturated Rh center supplies the pair of electrons to Os in order to balance the loss of CO from the complex, forming a Rh→Os dative bond as formulated above. This process can be viewed as an example of the anchimeric or neighboring group effect[45,46] in transition-metal chemistry, in which labilization of a carbonyl group on Os is promoted by electron donation from Rh. A similar effect was also proposed in the closely related species $[RhRe(CO)_4(\mu\text{-}RC\equiv CR)(dppm)_2]$.[6] Although the structures of 12 and 13 could also be formulated with "normal" Rh–Os covalent bonds and with the positive charge localized on Rh, as in the precursor, we favor the dative-bonded structure owing to the structure parameters obtained for the DMAD complex 12 (vide infra). In addition, this formulation gives Rh(I)/Os(II) centers instead of the Rh(II)/Os(I) states obtained in the covalent description; we suggest that the former is favored.

Support for our earlier suggestion, that ligand substitution in such complexes occurs by prior coordination of the incoming group at Rh, is obtained from reactions of 12 and 13 with some neutral and anionic groups. Com-

pound 12 reacts with isocyanides, iodide ion, and the dimethyldithiophosphinate anion to yield the species $[RhOs(CO)_2(L)(\mu\text{-}CO)(\mu\text{-}DMAD)(dppm)_2]^{n+}$ ($n = 1$, L = ^tBuNC (14), ^iPrNC (15); $n = 0$, L = I (16), S_2PMe_2 (17)).

14–18   21   19, 20, 22, 23
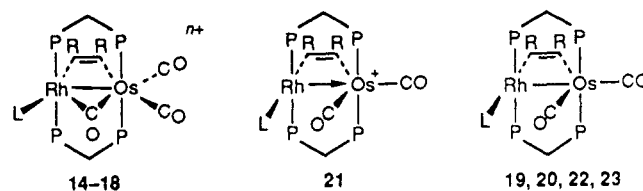
In all cases the $^{13}C\{^1H\}$ NMR spectra show two carbonyls bound solely to Os while the third is at lower field, typical of bridging carbonyls, and displays coupling to Rh of only ca. 20 Hz, which is substantially less than the 50–70 Hz obtained when a carbonyl is terminally bound to Rh. The IR spectra for these complexes also have a low-frequency carbonyl stretch (ca. 1700 cm^{-1}) that is typical for ketonic carbonyls.[41] The dithiophosphinate group is bound in a unidentate fashion as shown by the IR bands at 579 and 601 cm^{-1}, which appear typical for such a binding mode,[47] and by the ^{31}P chemical shift observed at δ 53.55, which is close to that of the free ligand (δ 54.03 in CD$_3$OD); when this group bridges two metals or chelates, the chemical shift is typically 30–50 ppm further downfield.[31,48] Compound 14 can also be prepared by reaction of the tetracarbonyl species 11 with ^tBuNC, with concomitant CO evolution. In this case the first product probably results from ^tBuNC coordination at the coordinatively unsaturated Rh center, followed by loss of a carbonyl.

Compound 13 also reacts with ^tBuNC to yield the tricarbonyl product $[RhOs(CO)_2(^tBuNC)(\mu\text{-}CO)(\mu\text{-}HFB)(dppm)_2][BF_4]$ (18), analogous to the above DMAD-bridged species. However, reactions of the anionic groups I$^-$ and S$_2PMe_2^-$ with 13 do not give the tricarbonyl products but instead yield the dicarbonyl species $[RhOsX(CO)_2(\mu\text{-}HFB)(dppm)_2]$ (X = I (19), S$_2PMe_2$ (20)) by carbonyl loss. The $^{13}C\{^1H\}$ NMR spectra of these products clearly indicate that both carbonyls are bound to Os, and the IR and $^{31}P\{^1H\}$ NMR spectra again indicate that the dithiophosphinate group is unidentate, leading to the structural formulation diagrammed earlier. In these HFB-bridged complexes it is not clear why carbonyl loss should be more facile with anionic ligands than with the neutral ^tBuNC group; we would have expected the opposite, since the neutral complexes resulting from anion coordination should bind carbonyls more effectively than the cationic species. Carbonyl loss can also be induced in $[RhOs(CO)_2L(\mu\text{-}CO)(\mu\text{-}DMAD)(dppm)_2]^{n+}$ ($n = 1$, L = ^iPrNC (15); $n = 0$, L = I (16), S$_2PMe_2$ (17)) by refluxing in THF, yielding $[RhOs(CO)_2L(\mu\text{-}DMAD)(dppm)_2]^{n+}$ ($n = 1$, L = ^iPrNC (21); $n = 0$, L = I (22), S$_2PMe_2$ (23)), and no doubt the other members of the series (14–18) can also readily lose CO to yield their dicarbonyl analogues, although these reactions were not attempted. These dicarbonyl complexes (19–23) are stoichiometrically analogous to compound 12 and so might be assumed to have a related structure in which there is a Rh(I)→Os(II) dative bond. However, a structure in which rhodium has a geometry analogous to that observed in $[Rh_2Cl_2(\mu\text{-}HFB)(dppm)_2]$,[49] giving a Rh(II) formulation, is another possibility. Although the rhodium geometry in this Rh$_2$ species

(42) Gagné, M. R.; Takats, J. *Organometallics* 1988, 7, 561.
(43) McDonald, R.; Cowie, M. To be submitted for publication.
(44) Kosower, E. M. *An Introduction to Physical Organic Chemistry*; Wiley: New York, 1968; p 49.
(45) Capon, B.; McManus, S. P. *Neighboring Group Participation*; Plenum: New York, 1976; Vol. 1.
(46) Capon, B. *Q. Rev., Chem. Soc.* 1964, 18, 45.

(47) Steele, D. F.; Stephenson, T. A. *J. Chem. Soc., Dalton Trans.* 1973, 2124.
(48) Sime, W. J.; Stephenson, T. A. *J. Chem. Soc., Dalton Trans.* 1978, 1647.
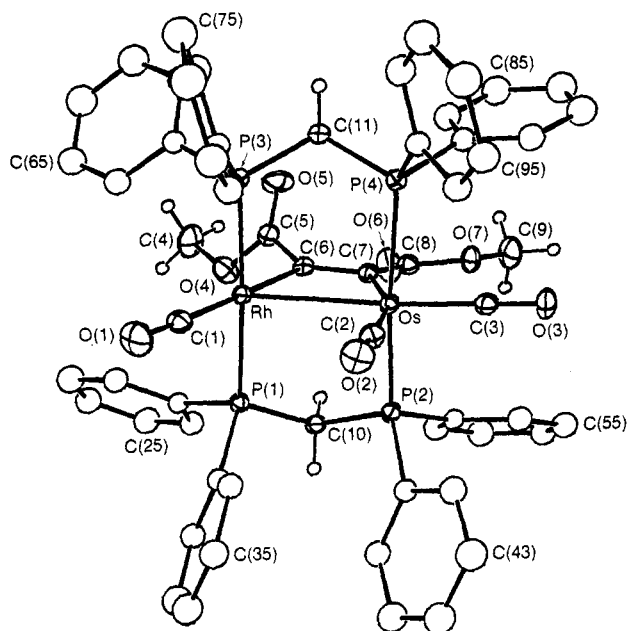(49) Cowie, M.; Dickson, R. S. *Inorg. Chem.* 1981, 20, 2682.

Figure 2. Perspective view of the [RhOs(CO)$_3$(μ-DMAD)-(dppm)$_2$]$^+$ cation of compound **12**. Thermal ellipsoids are shown at the 20% level except for hydrogens, which are either drawn arbitrarily small or omitted. Numbering on all phenyl carbons starts at the ipso carbon and moves sequentially around the ring.

is only subtly different from that in compound **12** (vide infra), we suggest that this has significant implications regarding the nature of the metal–metal interaction and the oxidation-state assignments for the metals. In this dirhodium complex both metals, which are in the +2 oxidation state, are distorted significantly from square planar owing to the Rh–Rh interaction, which can be viewed as a conventional covalent bond, yielding distorted-trigonal-bipyramidal (TBP) coordinations. In **12** the formation of the Rh→Os bond has not resulted in significant distortions from a square-planar Rh coordination (vide infra). As will be shown, this supports the dative bond formulation. We propose that compound **21**, in which the Rh-bound carbonyl group is replaced by the neutral ^{i}PrNC ligand, has a structure analogous to that of **12**. In such a structure the positive charge of the complex is localized on Os, giving favorable Rh(+1) and Os(+2) formulations. In compounds **19**, **20**, **22**, and **23**, however, the anionic I$^-$ and S$_2$PMe$_2^-$ groups attached to Rh result in Rh(+2) and Os(+1) formulations, requiring a covalent Rh–Os bond and a distorted TBP geometry at Rh, as observed previously for the Rh$_2$ species.[49] Support for the differing Rh oxidation states between [RhOs(CO)$_3$(μ-DMAD)(dppm)$_2$]-[BF$_4$] (**12**) and [RhOsI(CO)$_2$(μ-DMAD)(dppm)$_2$] (**22**) comes from the chemical shifts of the ^{103}Rh nuclei;[50] in compound **12** the Rh chemical shift (δ −508.6) appears characteristic of Rh(+1), whereas for compound **22** the value of δ +331.0 appears consistent with a Rh(+2) formulation.[51] The higher Rh oxidation state for the neutral species may explain the greater carbonyl lability noted above for these complexes.

Description of the Structure of Compound 12. The title compound crystallizes with two molecules of CH$_2$Cl$_2$

in the asymmetric unit. There are no unusual contacts between the complex cation, the solvent molecules, and the BF$_4^-$ anion, the last two of which have the expected geometries. A view of the complex cation is shown in Figure 2.

As suggested by the spectroscopic data, compound **12** has an approximate trans arrangement of the two bridging dppm groups with an accompanying cis-dimetalated arrangement of the DMAD group parallel to the metal–metal axis. The deviation of the P(2)–Os–P(4) and P(1)–Rh–P(3) linkages from linearity (163.54 (4) and 173.18 (4)°, respectively) results from the compression of the Rh–Os distance owing to metal–metal bond formation. Within the alkyne ligand the angles at C(6) and C(7) are close to 120°, showing sp^2 hybridization of these atoms, and the C(6)–C(7) distance of 1.321 (5) Å corresponds to a C=C double bond. These parameters are consistent with a cis-dimetalated olefin formulation for this group. The two CO$_2$Me substituents are skewed by 66° with respect to each other, such that one lies approximately in the metal–alkyne plane and the other is perpendicular to this plane. Such an arrangement appears typical for this ligand[41,52] and appears to minimize intramolecular steric interactions. Binding of the alkyne is somewhat unsymmetrical, being offset slightly toward Os. Although this offset does not show up noticeably in the metal–alkyne distances, with both being comparable, it is clearly shown in the angles at the alkyne carbons, with the Os–C(7)–C(6) angle being much more acute than Rh–C(6)–C(7) (102.7 (3) vs 120.9 (3)°). The offset may result from steric interactions, in which the phenyl groups 2 and 6 force the alkyne toward Os, or it may be that the DMAD group interacts more strongly with the third-row Os than with Rh; this effect would also be more pronounced in the present case since the proposed Rh→Os interaction (vide supra) should give rise to increased π back-donation to the alkyne from Os.

The geometry about Rh is almost exactly square planar, if one ignores the Rh–Os interaction, with both angles at Rh involving the mutually trans groups being close to 180°. This argues for a Rh→Os dative interaction since the presence of a "normal" Rh–Os covalent bond would be expected to result in the appropriate 5-coordinate hybridization at Rh. In donor–acceptor complexes, on the other hand, the donor atoms have been shown to retain the geometry they would have in the absence of the dative bond.[4,7,24,25,37,53–56] In contrast to this square-planar Rh coordination, the geometries at the Rh centers in the closely related species [Rh$_2$Cl$_2$(μ-HFB)(dppm)$_2$], in which there is a covalent Rh–Rh bond, are approximately trigonal bipyramidal.[49] At Os the geometry is significantly distorted from octahedral owing to the strain involving the bridging alkyne group and the Rh→Os bond. The carbonyl group opposite this bond (C(3)O(3)) is more strongly bound to Os than is the carbonyl cis to this interaction (C(2)O(2)), yielding Os–C distances of 1.859 (5) and 1.930 (4) Å, respectively. This is again consistent with the dative nature of the Rh→Os interaction, which apparently

(50) Von Philipsborn, W. *Pure Appl. Chem.* **1986**, *58*, 513.
(51) (a) Rhodium chemical shifts were obtained via ^{31}P detected indirect two-dimensional ^{31}P, ^{103}Rh{^{1}H} NMR spectroscopy (see: Elsevier, C. J.; Ernsting, J. M.; de Lange, W. G. J. *J. Chem. Soc., Chem. Commun.* **1989**, 585). (b) Full details of the use of ^{103}Rh chemical shifts to obtain information about the Rh oxidation states in related mixed-metal complexes will be published.

(52) Einstein, F. W. B.; Pomeroy, R. K.; Rushman, P.; Willis, A. C. *Organometallics* **1985**, *4*, 250.
(53) Iggo, J. A.; Markham, D. P.; Shaw, B. L.; Thornton-Pett, M. *J. Chem. Soc., Chem. Commun.* **1985**, 432.
(54) Breen, M. J.; Duttera, M. R.; Geoffroy, G. L.; Novotnak, G. C.; Roberts, D. A.; Shulman, P. M.; Steinmetz, G. R. *Organometallics* **1982**, *1*, 1008.
(55) Jacobsen, G. B.; Shaw, B. L.; Thornton-Pett, M. *J. Chem. Soc., Chem. Commun.* **1986**, 13.
(56) Targos, T. S.; Rosen, R. P.; Whittle, R. P.; Geoffroy, G. L. *Inorg. Chem.* **1985**, *24*, 1375.

strengthens the Os–carbonyl bond opposite the donor atom (Rh). This effect has been observed previously in related dative-bonded compounds.[25,38,52] The Rh–Os separation of 2.8744 (3) Å is typical of a single bond but is not a useful indication about the nature of this interaction, especially in the presence of the bridging alkyne. This Rh–Os bond is somewhat longer than that observed (2.758 (5) Å) in the related compound [RhOsCl$_2$Br(μ-CO)(dppm)$_2$],[53] which in our interpretation would have an Os→Rh donor–acceptor bond accompanied by semibridging carbonyl groups. The significant difference in these two Rh–Os distances no doubt results from the very different bridging ligands involved, with the alkyne group causing greater separation of the metals in the present case.

Summary

A series of low-valent, dppm-bridged complexes involving Rh and Os are readily obtained from [RhOsH(CO)$_3$(dppm)$_2$]. Carbonyl substitution in [RhOs(CO)$_4$(dppm)$_2$]$^+$ by the poorer π-acceptor but better σ-donor ^{t}BuNC ligand occurs on Os opposite the metal–metal bond, supporting our arguments that the Os–Rh bonds in these species are best regarded as donor–acceptor interactions. Carbonyl loss from the saturated Os center in the compounds [RhOs(CO)$_3$(μ-CO)(μ-RC≡CR)(dppm)$_2$][BF$_4$] is accompanied by the unusual formation of a Rh→Os dative bond, regenerating coordinative saturation at Os. This

may be viewed as an example of the neighboring-group effect, with Rh assisting in labilization of a carbonyl from Os. The presence of the coordinatively unsaturated Rh center in these compounds provides a route into chemistry involving the normally inert and coordinatively saturated Os center, and it is probable that substitution reactions occur by coordination at Rh, followed by facile rearrangement. This suggestion is supported by the reactions of [RhOs(CO)$_3$(μ-RC≡CR)(dppm)$_2$][BF$_4$] with a series of neutral and anionic ligands, in which the incoming ligands are clearly shown to be bound to the Rh center.

Supplementary Material Available: Listings of anisotropic thermal parameters, positional and thermal parameters for the BF$_4$$^-$ anion and CH$_2$Cl$_2$ molecules, additional bond lengths and angles, and hydrogen atom parameters for 12 and NMR data for 9–22 (11 pages); a listing of the observed and calculated structure factors for 12 (48 pages). Ordering information is given on any current masthead page.

Multiple Bonds between Main-Group Elements and Transition Metals. 77.[1] Condensation Reactions of Methyltrioxorhenium(VII) with Catechols and Aromatic Thiols

Janos Takacs,[2a] Malcolm R. Cook,[2b] Paul Kiprof, Josef G. Kuchler, and Wolfgang A. Herrmann*

Anorganisch-chemisches Institut der Technischen Universität München, Lichtenbergstrasse 4, D-8046 Garching bei München, Germany

The title compound methyltrioxorhenium(VII) reacts with catechols to yield complexes of the formula CH$_3$Re(O)$_2$(1,2-O$_2$C$_6$R$_4$) ((2)) that are fully characterized as pyridine adducts 3. Conducting these reactions in the presence of nucleophiles, e.g., halides, gives the hexacoordinate anions [CH$_3$Re(O)$_2$(1,2-O$_2$C$_6$R$_4$)(X)]$^-$ of compounds 4a–c (X = Cl, Br, I) in high yields. Based upon spectroscopic data, the oxo ligands occupy cis positions and the halide ligand occupies trans positions with respect to the methyl group of these novel five-membered d^0 rhenacycles. The rhenium(V) species "CH$_3$ReO$_2$", prepared in situ from 1 by reduction with (polymer bound) triphenylphosphane, reacts with phenanthrenequinone in the presence of pyridine to give the neutral hexacoordinate complex CH$_3$Re(O)$_2$(9,10-O$_2$C$_{14}$H$_8$)(NC$_5$H$_5$) (5), with the quinone ligand being present in the reduced form as catecholate while the rhenium is in the oxidation state VII. Reaction of 1 with thiophenol gives initially the rhenium(VII) complex CH$_3$ReO(SC$_6$H$_5$)$_4$ (6), which upon heating undergoes intramolecular elimination of diphenyl disulfide, C$_6$H$_5$SSC$_6$H$_5$, to give the dinuclear rhenium(V) complex [CH$_3$ReO(μ-SC$_6$H$_5$)(SC$_6$H$_5$)]$_2$ (7; X-ray diffraction study). Condensation of 1 with benzene-1,2-dithiol gives the rhenium(VII) complex CH$_3$ReO(1,2-S$_2$C$_6$H$_4$)$_2$ (8).

Introduction

Alkyl- and arylrhenium oxides represent an interesting class of compounds.[3] They have useful catalytic applications, with olefin oxidation and olefin metathesis being

typical, well-documented examples.[4] In these processes, especially, the title compound methyltrioxorhenium(VII) (1) acts as an effective catalyst. As part of our ongoing studies into the chemistry of this key compound, we recently reported on its condensation reactions with aromatic bidentate ligands of the type HO⋯X (X = N, NH$_2$, OH).[5] In the present account, we focus on condensation reactions with catechols; novel anionic rhenacycles are thus easily accessible. In addition, we report on condensation reac-

(1) For part 76 see: Herrmann, W. A.; Felixberger, J. K.; Kuchler, J. G.; Herdtweck, E. *Z. Naturforsch.* **1990**, *45B*, 876.

(2) (a) Alexander von Humboldt Fellow on leave from the Research Group for Petrochemistry of the Hungarian Academy of Sciences, Veszprem/Hungary. (b) Science and Engineering Research Council (U.K.) and NATO Postdoctoral Fellow (1988–1990).

(3) Reviews: (a) Herrmann, W. A. *Angew. Chem., Int. Ed. Engl.* **1988**, *27*, 1297; *Angew. Chem.* **1988**, *100*, 1269. (b) Herrmann, W. A. *Comments Inorg. Chem.* **1988**, *7*, 73. (c) Herrmann, W. A.; Herdtweck, E.; Flöel, M.; Kulpe, J.; Küsthardt, U.; Okuda, J. *Polyhedron* **1987**, *6*, 1165.

(4) Review: Herrmann, W. A. *J. Organomet. Chem.* **1990**, *382*, 1.

(5) Takacs, J.; Kiprof, P.; Riede, J.; Herrmann, W. A. *Organometallics* **1990**, *9*, 783.